


 Cite this: *RSC Adv.*, 2025, 15, 31683

Metal oxide-based heterogeneous acid catalysts for sustainable biodiesel synthesis: recent advances and key challenges

 Qiuyun Zhang,^{id}*^{ac} Jialu Wang,^{id}^c Xiaojuan Zhang,^{ac} Taoli Deng,^{ac} Yutao Zhang^{*,a} and Peihua Ma^{id}*^b

The synthesis of biodiesel is given wide attention due to its environmental benefits, renewability, and long-term sustainability. Importantly, it can also contribute to the elimination of the current global energy and climate change challenges. However, its production has been studied by the diverse catalytic systems. Metal oxide-based heterogeneous acid catalysts exhibit superior properties such as excellent reactivity, high thermal stability, resistance to free fatty acids and water, and reusability. Hence, the development of highly efficient and stable metal oxide-based heterogeneous acid catalysts is essential for future industrial applications. This review systematically explores recent developments in the production of biodiesel using metal oxide-based heterogeneous acid catalysts. The catalyst design and preparation, structural and physicochemical properties, operating reaction conditions, and catalytic behaviors of metal oxide-based heterogeneous acid catalysts, including sulfated metal oxide catalysts, different metal oxide-based acid catalysts, mixed metal oxide-based acid catalysts, and MOF-derived metal oxide-based acid catalysts, are discussed. Finally, the review concludes with guidance on the rational design of metal oxide-based heterogeneous acid catalysts for eco-friendly and cost-effective biodiesel production and puts forward the current research challenges and future development perspectives, aiming to promote innovation in large-scale industrial biodiesel production.

 Received 13th July 2025
 Accepted 21st August 2025

DOI: 10.1039/d5ra05017k

rsc.li/rsc-advances

1. Introduction

Fossil energy plays a critical role in the global economic, industrial and overall societal development. However, the global fossil energy consumption has been significantly increasing along with the population expansion, economic growth, rapid industrialization, and increasing rate of urbanization.¹ Moreover, the consumption of fossil fuels is also related to the rapid rise in CO₂ emissions, which is a major source of greenhouse gases and can cause substantial harm to ecosystems.^{2,3} Consequently, the development of renewable and clean biofuels has become the world's fastest-growing form of energy. Among these, biodiesel is widely recognized as the most promising option due to its renewable, non-toxic and biodegradable nature, low sulfur content, high flash point and cetane number, and high combustion efficiency.⁴⁻⁶

Currently, commercial biodiesel synthesis typically involves the esterification/transesterification reaction between free fatty acids and triglycerides using various oils, short-chain alcohols, and a suitable catalyst.^{7,8} In recent decades, biodiesel has been derived from first- to fifth-generation feedstock (first-generation feedstock: edible oils, second-generation feedstock: non-edible oils, third-generation feedstock: cultivated algae, fourth-generation feedstock: photobiological solar fuel cells, and fifth-generation feedstock: waste cooking oils). However, each has its own drawbacks, such as food security, environmental problems, and high investment.⁹ Meanwhile, the type of raw feedstock may dramatically affect the market price of biodiesel.¹⁰ Additionally, the choice of a suitable catalyst plays a significant role in accelerating reactions, determining the conversion and yield of biodiesel, and reducing the energy consumption. Fig. 1 shows the different types of catalytic systems used in biodiesel production.

Extensive literature indicates that the homogeneous acid/base catalysts of NaOH, KOH, HCl, and H₂SO₄ exhibit high reactivity and affordability in the production of biodiesel.¹¹ However, the separation of homogeneous catalysts from the reaction system is challenging, making the biodiesel product impure while producing significant amounts of acidic or alkaline wastewater.^{12,13} In addition, enzymatic catalysts have become more popular in recent years, but their prohibitive price

^aSchool of Chemistry and Chemical Engineering, Key Laboratory of Agricultural Resources and Environment in High Education Institute of Guizhou Province, Anshun University, Anshun, 561000, Guizhou, China. E-mail: sci_gyzhang@126.com; zyt0516@126.com

^bSchool of Chemistry and Chemical Engineering, Guizhou University, Guiyang, 550025, Guizhou, China. E-mail: phma@gzu.edu.cn

^cKey Laboratory of Bioenergy Conversion and Green Materials, Anshun University, Anshun, 561000, Guizhou, China



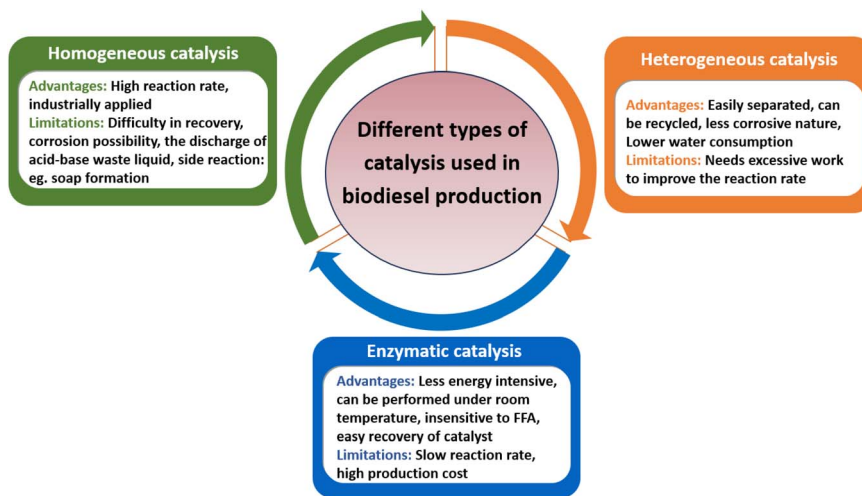


Fig. 1 Comparison of homogeneous catalysis, heterogeneous catalysis, and enzymatic catalysis.

is a major drawback.¹⁴ Recent advancements in heterogeneous catalysts (zeolites, heteropolyacids, carbon-based solid acids, metal-organic framework-based catalysts, *etc.*)^{15–17} with reusability and environmental friendliness, particularly those involving metal oxide-based heterogeneous acid catalysts, have shown potential results in addressing these limitations. Owing to the metal oxide-based heterogeneous acid catalysts' high structural and thermal stability, affordability, resistance to free fatty acids and water, and reusability,^{18,19} they are the ideal choice for sustainable biodiesel synthesis. However, a comprehensive understanding of various acidic metal oxide catalysts, including their design and synthesis, physicochemical properties, and catalytic performance, remains an important aspect for heterogeneous catalysis-based biodiesel production.

To the best of the authors' knowledge, some researchers have reviewed some recent developments in metal oxide-based catalysts to enhance biodiesel synthesis. In their separate reports, they mainly summarized the applications of CaO, MgO, and ZnO in biodiesel processing.^{20,21} Nevertheless, there is lack of a specific and timely analysis on the designs, structures, performances, and possible reaction mechanisms of metal oxide-based heterogeneous acid catalysts. Thus, it has become essential to provide a comprehensive update on the latest literature on this topic. In this context, the novelty of this review includes focusing on various metal oxide-based heterogeneous

acid materials, including sulfated metal oxide catalysts, different metal oxide-based acid catalysts, and mixed metal oxide-based acid catalysts, in biodiesel generation, in addition to bringing together the most recent works regarding the biodiesel production catalyzed by MOF-derived metal oxide-based catalysts. It provides a comprehensive summary of the catalyst design and preparation, structural and physicochemical properties, optimization of reaction conditions, catalytic behavior, and catalytic mechanism. Additionally, the review suggests current research challenges and future research directions and encourages further exploration of metal oxide-based heterogeneous acid catalysts. We hope that this review provides insights into the development of more efficient and sustainable heterogeneous acid materials.

2. Homogeneous acid catalysts for biofuel synthesis

Currently, homogeneous acid catalysts, such as HCl, H₂SO₄, and H₃PO₄, are used to catalyze esterification reactions. Meanwhile, a two-step process consisting of acid-catalyzed esterification, followed by alkali-catalyzed transesterification, has also been widely reported for producing biodiesel from low-cost feedstock with high free fatty acid (FFA) content. Table 1 reviews the production of biodiesel by homogeneous acid

Table 1 Comprehensive list of homogeneous acid catalysts for the biodiesel production process^a

Entry	Feedstock + alcohol	Catalyst	Conditions (time, temp., catalyst loading, molar ratio (acid (oil) : alcohol))	Yield (Y%)/conversion (C%)	Ref.
1	Mealworm oil + methanol	H ₂ SO ₄	174 min, 74 °C, 5.8%, 1 : 24	C = 92.74 ± 0.92	23
2	High-acidity animal fats + methanol	H ₂ SO ₄	2 h, 65 °C, 0.5%, 1 : 6	C = 88.8	24
3	<i>Hevea brasiliensis</i> seed + methanol	H ₂ SO ₄	45 min, 45 °C, 1.5%, 1 : 12	C = 99.55	25
4	Oleic acid + methanol	H ₂ SO ₄	30 min, RT, 0.7 mol L ⁻¹ , 1 : 12	C = 96.1 ± 0.4	26
5	Waste cooking oil + methanol	H ₂ SO ₄	40 min, 60 ± 5 °C, 2.6%, 1 : 10	C = 67.8	27

^a Catalyst amount: relative to the weight of the oil feedstock; room temperature: RT.



catalysts in recent years. As shown in the table, homogeneous acid catalysts are able to effectively catalyze esterification in a reasonably short time and at room temperature with high conversions, and the drawbacks of this acid-catalyzed process include producing relatively high levels of wastewater, complicated purification processes, and high prices of catalysts, which increase the cost of biodiesel production.²² Thus, heterogeneous acid-catalyzed esterification for biodiesel production is recommended.

3. Metal oxide-based heterogeneous acid catalysts

Thanks to their abundance, affordability, and distinctive characteristics, various metal oxide catalysts have gained attention among heterogeneous acid catalysts for producing biodiesel. They demonstrate excellent catalytic performance, high thermal stability, resistance to free fatty acids and water, and reusability, potentially addressing the drawbacks of conventional homogeneous acid catalysts. Thus, the recent advancements in the application of sulfated metal oxide catalysts, different metal oxide-based acid catalysts (silica-based catalysts, molybdenum oxide-based catalysts, tungsten oxide-based catalysts, tin oxide-based catalysts, iron oxide-based catalysts, aluminum oxide-based catalysts, titania-based catalysts, and zirconium-based catalysts), mixed metal oxide-based acid catalysts, and MOF-derived metal oxide-based catalysts in the synthesis of biodiesel are discussed thoroughly. Meanwhile, Table 2 presents the advantages and limitations of different metal oxide-based heterogeneous acid catalysts.

3.1 Sulfated metal oxide catalysts

Recently, the incorporation of the sulfate group into metal oxides, like sulfated metal oxides $\text{SO}_4^{2-}/\text{M}_x\text{O}_y$ ($\text{M} = \text{Ti}, \text{Zr}, \text{Sn},$ and Fe), which belong to the category of solid superacids due to the presence of Brønsted and Lewis acid sites, good mechanical and chemical stability, is receiving wide attention.²⁸ Hossain *et al.*²⁹ synthesized sulfonated zirconium oxide on SBA-15 ($\text{S-ZrO}_2/\text{SBA-15}$) by the direct impregnation method and then calcined it at 550 °C for 4 h. The catalyst was tested for biodiesel synthesis from hydrolyzed waste cooking oil under subcritical

methanol conditions. It was found that a yield of 96.383% was acquired within 10 min under the conditions of 140 °C, 2.0% catalyst, and 10 : 1 methanol-to-oil ratio. $\text{S-ZrO}_2/\text{SBA-15}$ showed good reusability, and its yield after five times of reuse was 90%. Using H_2SO_4 as an acid agent, Aneu *et al.*³⁰ prepared a solid acid catalyst, SO_4/SiO_2 , for the esterification of waste cooking oil. The SO_4/SiO_2 catalyst calcined at 550 °C showed high acidity (0.97 mEq KOH per g) and the best catalytic activity and could reduce the FFA content from 3.6% to 1.62% with 5% of the catalyst amount, 1 : 23 molar ratio of waste cooking oil to methanol, and 1 h of reaction time. In another study, Utami and co-workers³¹ used impregnation and hydrothermal methods to synthesize a Cr-incorporated sulfated zirconia ($\text{Cr/ZrO}_2\text{-SO}_4$) solid catalyst for the conversion of palm oil into biofuels. The results showed that the non-calcined $\text{Cr/ZrO}_2\text{-SO}_4$ catalyst resulted in higher activity and selectivity than the calcined $\text{Cr/ZrO}_2\text{-SO}_4$ catalyst due to its higher acidity (2.33 mmol g^{-1}). Yusuf *et al.*³² synthesized β -zeolite, ZnO- β -zeolite, and sulfated-zinc oxide supported on β -zeolite ($\text{SO}_4^{2-}/\text{ZnO-}\beta\text{-zeolite}$) for biodiesel synthesis from waste cooking oil. The $\text{SO}_4^{2-}/\text{ZnO-}\beta\text{-zeolite}$ catalyst exhibited higher reaction conversion than β -zeolite and ZnO- β -zeolite, producing 96.9% biodiesel under optimal conditions, and the plausible mechanism for simultaneous transesterification and esterification was proposed (Fig. 2). The high catalytic activity was attributed to its large pore size (6.5 nm) and high acidity ($250.26 \text{ m}^2 \text{ g}^{-1}$). More importantly, the properties of the waste cooking oil-derived biodiesel met the ASTM6751 standard specification.

Hassan *et al.*³³ reported the application of a silica-supported solid superacid catalyst ($\text{S}_2\text{O}_8^{2-}/\text{TiO}_2\text{-SiO}_2$) as a heterogeneous acid catalyst in the production of biodiesel from waste culinary oil. Notably, $\text{S}_2\text{O}_8^{2-}/\text{TiO}_2\text{-SiO}_2$ outperformed the $\text{S}_2\text{O}_8^{2-}/\text{TiO}_2$ catalyst with a higher FFA conversion of 90.7% using 5 wt% of the catalyst amount, 12 : 1 molar ratio of methanol to oil, and 180 °C for 4 h of reaction time. The introduction of the sulfate group in metal oxides can achieve a superacid catalyst, which offers the superacidic properties (Brønsted and Lewis acid sites), thereby providing an important biodiesel output. However, sulfated metal oxides tend to deactivate after the reaction, resulting in the life cycle of such sulfated metal oxides not being as long as we expected.³⁴ Based on these points, the as-synthesized sulfated metal oxide catalysts still require deep

Table 2 Comparison of the advantages and limitations of different metal oxide-based heterogeneous acid catalysts

Catalyst	Advantages	Limitations
Sulfated metal oxide catalysts	Simple synthesis method, stronger Brønsted and Lewis acid sites	Leaching of sulfate ion species, coking and carbon deposition on the catalyst surface
Metal oxide-based acid catalysts (silica-based, molybdenum oxide-based, and tungsten oxide-based)	High thermal and chemical stability, high mechanical properties, ease of functionalization, adjustable redox properties	Scalability of production, weak interactions, lower catalyst activity
Mixed metal oxide-based acid catalysts	High thermal and chemical stability, high surface area, multiple active sites, good catalyst activity	Complex synthesis process, scalability of production, weak interactions
MOF-derived metal oxide-based catalysts	High porosity, high internal surface area, tunable pore size, multiple active sites, good catalyst activity	Complex synthesis process, long synthesis time, high cost, pore collapse



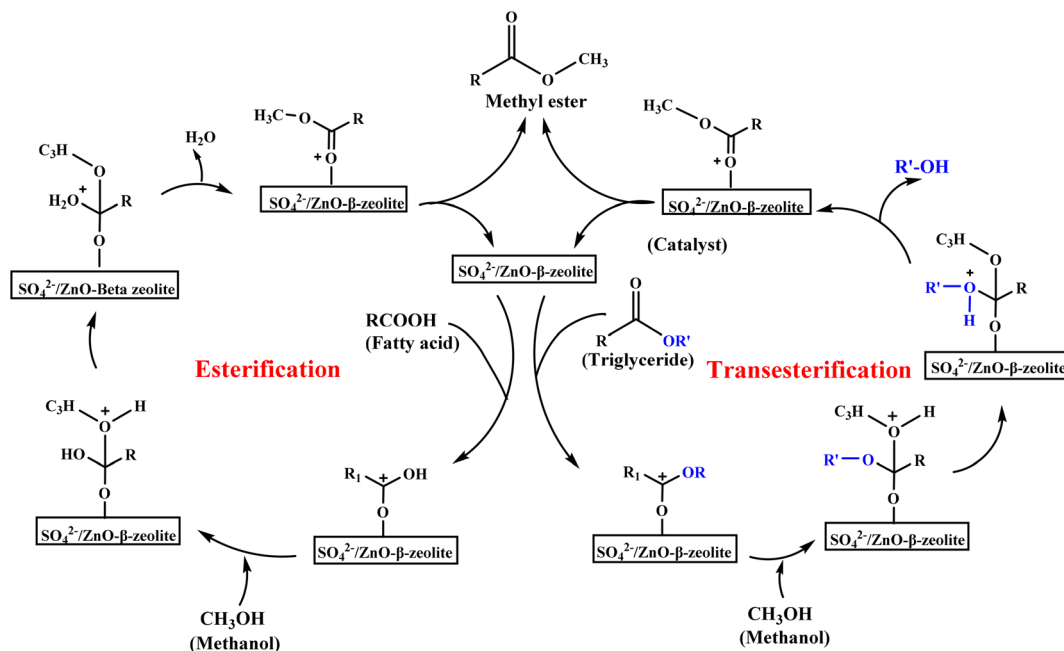


Fig. 2 Plausible mechanism for the concurrent esterification and transesterification reactions by $\text{SO}_4^{2-}/\text{ZnO}-\beta$ -zeolite. Ref. 32, reprinted with permission of copyright© (2023) open-access from the American Chemical Society.

investigation of their process optimizations and probable structure defects, which will be important for meeting industry standards and application requirements in the production of biofuels.

3.2 Various metal oxide catalysts

3.2.1 Silica-based catalysts. Silica-based materials (mesoporous silica, sulfonic acid-modified silica, and silica complexes) find applications in various fields like catalysis, energy storage, and adsorption and in different multidisciplinary fields because of their high surface area, high mechanical, tunable porosity/surfaces, and good thermal stability.³⁵ Meanwhile, silica-based catalysts are some of the supports or precursors used for biodiesel generation.

Recently, acid (sulfuric acid and chlorosulfonic acid)-functionalized silica has been recognized in the esterification/transesterification of FFAs. Changmai *et al.*³⁶ reported a magnetic $\text{Fe}_3\text{O}_4@/\text{SiO}_2-\text{SO}_3\text{H}$ core@shell catalyst by stepwise

co-precipitation, coating, and functionalization. It was found that $\text{Fe}_3\text{O}_4@/\text{SiO}_2-\text{SO}_3\text{H}$ had a magnetic saturation of 30.94 emu g^{-1} and a higher sulfonic acid loading. The conversion of the *Jatropha curcas* oil to biodiesel was 81% after the ninth cycle, comparable to the fresh catalyst. The TEM image of the recovered catalyst showed that the core@shell structure of $\text{Fe}_3\text{O}_4@/\text{SiO}_2-\text{SO}_3\text{H}$ remained intact. The kinetic study of the reaction showed that a 37 kJ mol^{-1} activation energy was required for the transesterification and esterification of *Jatropha curcas* oil. Saleh *et al.*³⁹ developed a heterogeneous acid nanocatalyst $\text{TiFe}_2\text{O}_4@/\text{SiO}_2-\text{SO}_3\text{H}$ for biodiesel production from oleic acid and palmitic acid. The activity test results of the catalyst revealed that $\text{TiFe}_2\text{O}_4@/\text{SiO}_2-\text{SO}_3\text{H}$ had high activity for the esterification. Also, the catalyst was utilized for four successive cycles without any loss of activity. In another study, Ghasemzadeh *et al.*⁴¹ developed a magnetic catalyst (cotton/ $\text{Fe}_3\text{O}_4@/\text{SiO}_2@-\text{H}_3\text{PW}_{12}\text{O}_{40}$) by the impregnation method and reported its catalytic performance for the production of biodiesel from sunflower oil with a biodiesel yield of 95.3% under optimal

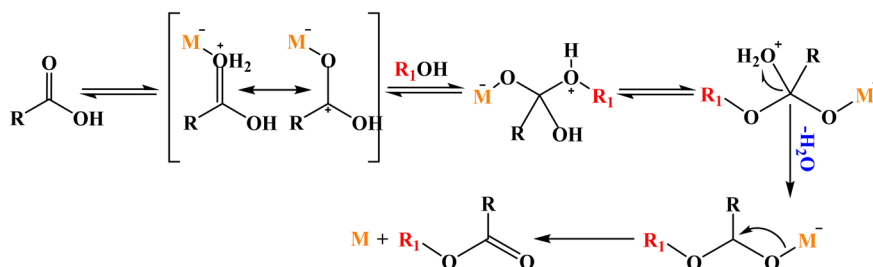


Fig. 3 Plausible mechanism for esterification using the $\text{CuS}-\text{FeS}/\text{SiO}_2$ catalyst. Ref. 48, reprinted with permission of copyright© (2022) open-access from MDPI.



Table 3 Comprehensive list of silica-based catalysts for the biodiesel production process^a

Entry	Feedstock + alcohol	Catalyst	Characterizations	Conditions (time, temp., catalyst loading, molar ratio (acid (oil) : alcohol))	Yield (Y%)/conversion (C/Y)	Reusability (run: C/Y)	Ref.
1	<i>Jatropha curcas</i> oil + methanol	Fe ₃ O ₄ @SiO ₂ -SO ₃ H	SA = 32.88, PD = 3.48, CA = 0.76	3.5 h, 80 °C, 8%, 1 : 9	C = 98 ± 1	9 runs: 81	36
2	Oleic acid + methanol	SiO ₂ NPs10_CSPTMS	N.R.	2 h, 120 °C, 10%, oleic acid (2 g); methanol (8.67 cm ³)	C = 100	6 runs: >20	37
3	Oleic acid + methanol	C-SOH	SA = 1464, PD = 4.95, CA = 1.55	8 h, 60 °C, 0.075 g, 1 : 40	C = 92	3 runs: >50	38
4	Oleic acid + methanol	TiFe ₂ O ₄ @SiO ₂ -SO ₃ H	SA = 21.01, PV = 0.15, PD = 16, CA = 8.9	1.5 h, 60 °C, 0.02 g, 2 : 9	Y = 97	4 runs: 96	39
5	Oleic acid + methanol	La-PW-SiO ₂ /SWCNTs	SA = 3.107, PV = 0.002, PD = 1.246, CA = 1.24	8 h, 65 °C, 1.5%, 1 : 15	C = 93.1	6 runs: 88.7	40
6	Sunflower oil + methanol	Cotton/	SA = 16.63, PV = 0.0917	3.5 h, 70 °C, 3%, 1 : 12	Y = 95.3	4 runs: 85.5	41
7	Oleic acid + ethanol	Fe ₃ O ₄ @SiO ₂ @H ₃ PW ₁₂ O ₄₀ HPW/MPN@SiO ₂	SA = 54, PV = 0.15, PD = 12, CA = 0.14	1 h, 100 °C, 10%, 1 : 6	C = 98	4 runs: 97	42
8	Oleic acid + ethanol	Fe ₃ O ₄ @SiO ₂ @PIL	N.R.	4 h, 90 °C, 9.5%, 1 : 11.5	Y = 92.1	6 runs: 89.2	43
9	Cooking oil + methanol	Fe ₃ O ₄ @SiO ₂ -APTES-L ^{AE} -Mo ^V O ₂	SA = 69.048, PD = 6.95, CA = 3.162	0.75 h, RT, 0.04 g, 1 : 3	C = 99	12 runs: 92	44
10	Palmitic acid + methanol	Fe ₃ O ₄ @SiO ₂ -P[(VLM)]PW	CA = 3.8	6 h, 70 °C, 10%, 1 : 12	C = 94	5 runs: 84	45
11	Rice bran oil + methanol	ZnO/SiO ₂ -25	SA = 82.8, PV = 0.048, PD = 0.95, CA = 1.34	4 h, 100 °C, 6 g L ⁻¹ , 1 : 8	C ≈ 100	5 runs: ≈ 90	46
12	Palm fatty acid distillate + methanol	NiSO ₄ /SiO ₂	SA = 10.1919, PV = 0.045257, PD = 17.7617	7 h, 110 °C, 15%, 1 : 5	C = 93	2 runs: 79.85	47
13	Palm fatty acid distillate + methanol	CuS-FeS/SiO ₂	SA = 40, PV = 0.57, CA = 4.13329	3 h, 70 °C, 2%, 1 : 15	C = 98	5 runs: 82.73	48
14	Low-value acidic oils + methanol	MoAl@H-SiO ₂	SA = 458.1, PV = 0.17, PD = 2.66, CA = 3.56	8 h, 130 °C, 8%, 1 : 35	C = 94.27	5 runs: 81.81	49

^a SA (surface area): m² g⁻¹; PV (pore volume): cm³ g⁻¹; PD (pore diameter): nm; CB (catalyst basicity): mmol g⁻¹; CA (catalyst acidity): mmol g⁻¹; not reported: N.R.; catalyst amount: relative to the weight of the oil feedstock; room temperature: RT.

conditions, and the yield was higher than 85% after using for four times. Further, the quality of the sunflower biodiesel product satisfied international ASTM D-6751 and EN-14214 standards, and it could be accepted for commercial production and applications.

A heterogeneous CuS–FeS/SiO₂ catalyst derived from rice husk silica for the synthesis of biodiesel from the Malaysian palm fatty acid distillate was reported by Albalushi *et al.*⁴⁸ Under optimum conditions, the conversions exceeded 98%, and its excellent activity was ascribed to the increased active site acidity levels. Moreover, the suggested mechanism of esterification catalyzed by CuS–FeS/SiO₂ catalyst is presented in Fig. 3. A summary comparing silica-based catalysts for the biodiesel production process is tabulated, as shown in Table 3. As shown in Table 3, the good yield/conversion of biodiesel products has been obtained using various silica-based catalysts; however, the search for new silica-based catalysts with excellent catalytic activity and stability for biofuel generation on an industrial scale is also suggested.

3.2.2 Molybdenum oxide-based catalysts. Among the various metal oxide catalysts, it is possible to highlight molybdenum oxide-based catalysts due to its excellent catalytic, optics, and gas sensor, stronger Brønsted and Lewis acidic, and adjustable redox properties, can be widely used in various multidisciplinary fields. In a study reported by Sabzevar *et al.*,⁵¹ the application of α -MoO₃ nanobelts in a straightforward procedure for biodiesel synthesis was examined, presenting an ester yield of 85% under optimal conditions. In addition, the prepared α -MoO₃ catalyst could be easily recycled with slightly decreased activity. In another similar study, Chaudhry *et al.*⁵² synthesized a MoO₃ nanocatalyst by the *in situ* wet impregnation approach from *Ipomoea* seed shells. Further, this MoO₃ nanocatalyst was exploited for its efficacy in the production of biodiesel from the inedible oil seeds of *Ipomoea cairica*. It was reported that MoO₃ exhibited promising catalytic activity, showing a ~95% biodiesel yield at 50 °C within 2 h.

de Brito *et al.*⁵³ reported a wet impregnation method to synthesize a new solid catalyst MoO₃/Nb₂O₅. In their study, the MoO₃/Nb₂O₅ catalyst revealed high catalytic performance for biodiesel (conversion = 94.2%). Moreover, the catalytic activity of the catalyst slightly decreased in cycles 6 and 7, with conversions of 86.8% and 82.7%, respectively, and, importantly, decreased after the 8th cycle due to the obstruction of the acid sites by the deposit of organic materials. In addition, the kinetic analysis showed that the activation energy and Gibbs free

energy for the transesterification reaction of waste frying oil in this study were 32.00 kJ mol⁻¹ and 118.02 kJ mol⁻¹, respectively, indicating that this system had a non-spontaneous and endergonic nature. da Silva *et al.*⁵⁷ studied the catalytic activity of the MoO₃/GO catalyst, in which molybdenum oxide was supported over graphene oxide. MoO₃/GO proved to be a high-acid material with a surface acidity value of 14.2 mmol H⁺ per g. Meanwhile, the simultaneous esterification and transesterification of waste cooking oil were performed in the presence of the catalyst. A conversion of 95.6% was obtained under ideal conditions. However, the conversion of this reaction decreased from 95.6% to 36.6% after reusing for 7 times, and it was confirmed to be related to leaching on the catalyst surface (MoO₃ species). In another study, a two-dimensional graphitic carbon nitride-supported molybdenum catalyst (*x*Mo/g-C₃N₄) was prepared by an incipient wet impregnation method (Fig. 4). Waste cooking oil was transesterified on a 10% Mo/g-C₃N₄ catalyst, with a conversion of up to 71.1%, and the catalyst was used only one time due to significant catalyst activity loss.⁵⁸

Recently, there has been a great interest in the use of molecular sieves with high surface areas to support molybdenum oxide. Zhang *et al.*⁵⁹ synthesized the Mo(vi) oxide species incorporated on the outer surface of ZSM-22 through the wet impregnation method for biodiesel synthesis and achieved a conversion of 59.29%. Cavalcante *et al.*⁶¹ evaluated a mesoporous molecular sieve MCM-41 catalyst incorporated with MoO₃ in the transesterification of corn oil under ideal conditions and achieved a maximum yield of 87.87%. Interestingly, the characterization results clearly demonstrated that the molybdenum formed bonds in the MoO₃/MCM-41 catalyst and the migration of the active phase of MoO₃/MCM-41 with 20 wt% MoO₃ to the micro- and mesopores hindered the chemical interactions at the active surface.

Gonçalves and co-workers⁶⁴ synthesized and evaluated the magnetic acid catalyst MoO₃/SrFe₂O₄ for the production of biodiesel from waste cooking oil. Based on the characterizations, MoO₃ was successfully anchored on the magnetic SrFe₂O₄ support and possessed bifunctional characteristics (catalytic and magnetic). The MoO₃/SrFe₂O₄ catalyst achieved a maximum biodiesel conversion of 95.4% under optimal reaction conditions. Subsequently, nickel ferrite (NiFe₂O₄) impregnated with MoO₃ was prepared and applied in the methyl transesterification reaction of waste cooking oil.⁶⁵ As a result, a conversion of 95.6% was obtained under ideal conditions, and the MoO₃/SrFe₂O₄ catalyst showed high

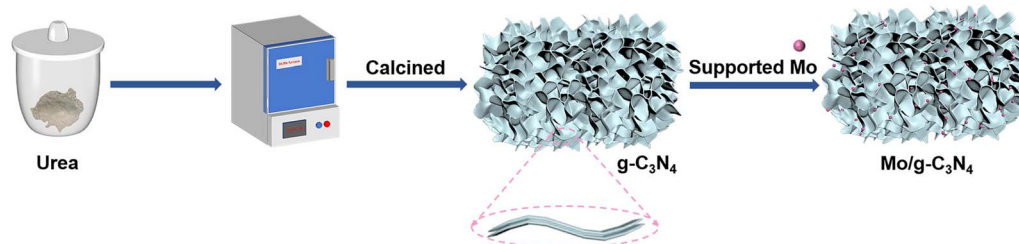


Fig. 4 Synthesis process of the Mo/g-C₃N₄ catalyst. Ref. 58, reprinted with permission of copyright© (2023) from Elsevier.



Table 4 Comprehensive list of molybdenum oxide-based catalysts for the biodiesel production process^a

Entry	Feedstock + alcohol	Catalyst	Characterizations	Conditions (time, temp., catalyst loading, molar ratio (acid (oil) : alcohol))	Yield (Y%)/conversion (C%)	Reusability (run: C/Y)	Ref.
1	Oleic acid + methanol	MoO ₃ -10	SA = 10.2, PD = 37.79	5 h, 120 °C, 5%, 1 : 10	C = 97.2	9 runs: 87.1	50
2	Oleic acid + ethanol	α-MoO ₃	Not reported	28 min, 75 °C, 0.001 g, 1 : 30	Y = 76	4 runs: 67.41	51
3	<i>Ipomoea cairica</i> L. seeds + methanol	MoO ₃	Not reported	2 h, 50 °C, 0.4%, 1 : 15	Y = 95	5 runs: 90.6	52
4	Low-quality oil + methanol	MoO ₃ /ZrO ₂ /KIT-6	SA = 612.85, PV = 1.11, PD = 7.25, CA = 0.756	12 h, 130 °C, 12%, 1 : 20	C = 92.7	5 runs: 85.7	53
5	<i>Jatropha</i> seed oil + methanol	10Mo/1.5ST	SA = 70, PV = 0.23, PD = 11.3, CA = 30.28	16 h, 110 °C, 3%, 1 : 9	C = 89.3	5 runs: 75.2	54
6	Waste frying oil + methanol	30-MoO ₃ /Nb ₂ O ₅	SA = 10.906, PV = 0.028, PD = 10.365	2.5 h, 145 °C, 6%, 1 : 20	C = 94.2	8 runs: 72	55
7	Rapeseed oil + methanol	Fe ₃ O ₄ @SiO ₂ -APTESMoO ₂ L ₂ ^{DHAPb}	CA = 0.30811	2 h, RT, 0.1%, 1 : 3	C = 97	12 runs: 85	56
8	Waste cooking oil + methanol	MoO ₃ /GO	CA = 14.2	5 h, 140 °C, 6%, 1 : 35	C = 95.6	7 runs: 36.6	57
9	Waste cooking soybean oil + methanol	10Mo/g-C ₃ N ₄	SA = 65, PV = 0.28	12 h, 120 °C, 2%, 1 : 9	C = 71.1	1 runs: 53.8	58
10	Waste cooking soybean oil + methanol	5Mo/ZSM-22	SA = 149, PV = 0.18	12 h, 120 °C, 0.06, 1 : 9	C = 59.29	4 runs: 58.38	59
11	Soybean oil + methanol	10% MoO ₃ /Al-SBA-15	SA = 311.08, PV = 0.51, PD = 8.083	3 h, 150 °C, 3%, 1 : 20	Y = 96	5 runs: 62	60
12	Corn oil + methanol	MoO ₃ /MCM-41	SA = 186.74, PV = 0.11, PD = 4.285, CA = 0.01	3 h, 150 °C, 3%, 1 : 20	Y = 87.87	N.R.	61
13	Soybean oil + methanol	6-MoO ₃ /H-Z/S	SA = 304.24, PV = 0.16, PD = 2.813, CA = 0.001	4 h, 150 °C, 3%, 1 : 20	Y = 79.2	N.R.	62
14	<i>Abrus precatorius</i> oil + methanol	MoO ₃ -HPW/Ga-KIT-6	SA = 678, PV = 0.65, PD = 6.4, CA = 0.3413	3 h, 100 °C, 0.2 g, 1 : 6	Y = 100	5 runs: 96	63
15	Waste cooking oil + methanol	MoO ₃ /SrFe ₂ O ₄	CA = 7.12	4 h, 164 °C, 10%, 1 : 40	C = 95.4	5 runs: 84	64
16	Waste cooking oil + methanol	30-MoO ₃ /NiFe ₂ O ₄	CA = 8.8	1 h, 168 °C, 10%, 1 : 30	C = 95.4	7 runs: 90.3	65

^a SA (surface area): m² g⁻¹; PV (pore volume): cm³ g⁻¹; PD (pore diameter): nm; CB (catalyst basicity): mmol g⁻¹; CA (catalyst acidity): mmol g⁻¹; not reported: N.R.; catalyst amount: relative to the weight of the oil feedstock; room temperature: RT.

stability and versatility in the presence of various raw materials with different acidity indices. Table 4 shows the works on biodiesel production under different conditions using molybdenum oxide-based catalysts. As shown in the table, molybdenum oxide-based catalysts have been widely used in the production of biodiesel because of their abundance in nature, the water-tolerant nature of their Brønsted and Lewis acid sites, and their non-hazardousness. However, a major problem is developing scalable preparation methods that ensure molybdenum oxide's phase purity, crystallinity, and reproducibility. Thus, this requires interdisciplinary efforts spanning catalyst preparation, characterization, and environmental assessment.

3.2.3 Tungsten oxide-based catalysts. Due to its strong acidity from Brønsted acid sites (associated with the hydroxyl groups formed by terminal W–O bonds on the surface) and Lewis acid sites (related to the coordinatively unsaturated W^{6+} species), tungsten oxide has superb catalytic activity in various acid-catalyzed reactions. However, few literature studies have focused on the synthesis of biodiesel using tungsten oxide-based catalysts. Here, Table 5 presents the works on biodiesel synthesis using tungsten oxide-based catalysts. Mansir *et al.*⁶⁶ investigated the acid–base bi-functional tungsten–zirconia (W–Zr)-modified waste shell catalyst (WO_3 – Zr_2O_3 /CaO) for biodiesel synthesis from waste-based vegetable oil and declared that the bi-functional catalyst had a high catalytic performance, which may be ascribed to the distribution of appropriate acid density sites over the CaO support needed for simultaneous transesterification and esterification, and the high dispersion of WO_3 – Zr_2O_3 over the CaO support gave an appropriate surface area for transesterification. More importantly, the catalytic activity of WO_3 – Zr_2O_3 /CaO showed only a minor reduction after the fifth cycle of use. dos Santos *et al.*⁶⁷ recently tested the catalytic performance of the magnetic acid catalyst WO_3 /CuFe₂O₄ synthesized by a wet impregnation method in biodiesel production from waste cooking oil and observed a 95.2% biodiesel yield under ideal reaction conditions, and the catalyst could be recycled for five reaction runs. Interestingly, the biodiesel obtained was found in accordance with the ASTM

limits. Hsu *et al.*⁶⁹ reported a photolysis-free radical polymerization route for preparing a high-activity PPy/ZnFe₂O₄– WO_3 nanocomposite. Based on the experimental results, the transesterification reaction of olive oil was performed under milder conditions to reach a 94% yield. Meanwhile, the PPy/ZnFe₂O₄– WO_3 catalyst exhibited high stability for up to five runs with a lower performance loss. Importantly, the CO₂-TPD tests showed the excellent activity originating from its higher strength of basicity. Based on the literature, tungsten oxide-based catalysts are effective catalysts in the production of biodiesel. Whereas, the design of new synthesis strategies to build a stronger interaction between tungsten oxide and other species should be highlighted, resulting in favor of the catalytic activity of tungsten oxide-based catalysts.

3.2.4 Tin oxide-based catalysts. Owing to their abundant acid sites and oxidizing and reducing surface properties, the use of tin oxide and tin oxide-based materials has been attracting attention. Ibrahim *et al.*⁷¹ studied biodiesel production through the use of bifunctional SnO₂/ZrSiO₄ as a catalyst. The obtained characterization results showed the formation of rutile-SnO₂ and zircon in the composite, and the SnO₂/ZrSiO₄ catalyst possessed a good morphology with a mesoporous structure and different acidic properties. Additionally, the activity results revealed that the biodiesel yield in the esterification reaction of palmitic acid was 90.2% under optimum conditions, and the mechanism of the esterification reaction in the presence of SnO₂/ZrSiO₄ active sites is displayed in Fig. 5. Interestingly, the transesterification of soybean oil over SnO₂/ZrSiO₄ afforded an 88% biodiesel yield under the following reaction conditions: 70 °C, 4 h, 6.0% catalyst, and 1 : 10 oil : methanol ratio.

Prestigiacomo *et al.*⁷³ developed a molecular-colloidal coassembly route combined with an ultrasonic-assisted precipitation approach to prepare a cyclodextrin-derived SnO@ γ -Al₂O₃ composite. Characterization results revealed that the synergy of the template materials and γ -Al₂O₃ nanoparticles may have a synergistic effect on the growth and orientation of SnO microcrystals. Specifically, the as-prepared SnO@ γ -Al₂O₃ catalyzed the reaction with a biodiesel yield of 33.5% from rapeseed

Table 5 Comprehensive list of tungsten oxide-based catalysts for the biodiesel production process^a

Entry	Feedstock + alcohol	Catalyst	Characterizations	Conditions (time, temp., catalyst loading, molar ratio (acid (oil) : alcohol))	Yield (Y%/ conversion (C%))	Reusability (run: C/Y)	Ref.
1	Unrefined palm-derived waste oil + methanol	WO_3 – Zr_2O_3 /CaO	SA = 9.7, PV = 0.16, PD = 64.82, CA = 7.023, CB = 1.536	1 h, 80 °C, 2%, 1 : 15	Y = 94.1	5 runs: 79.3	66
2	Waste cooking oil + methanol	WO_3 /CuFe ₂ O ₄	CA = 7.43	3 h, 180 °C, 6%, 1 : 45	Y = 95.2	5 runs: 80.6	67
3	C3–C16 free fatty acids + methanol	WO_x /ZrO _x /PMO	CA = 0.5	6 h, 60 °C, 0.025 g, 1 : 30	C = 90	—	68
5	Olive oil + methanol	PPy/ZnFe ₂ O ₄ – WO_3	—	2 h, 55 °C, 3%, 1 : 14	Y = 94	5 runs: 90	69

^a SA (surface area): m² g^{−1}; PV (pore volume): cm³ g^{−1}; PD (pore diameter): nm; CB (catalyst basicity): mmol g^{−1}; CA (catalyst acidity): mmol g^{−1}; not reported: N.R.; catalyst amount: relative to the weight of the oil feedstock; room temperature: RT.



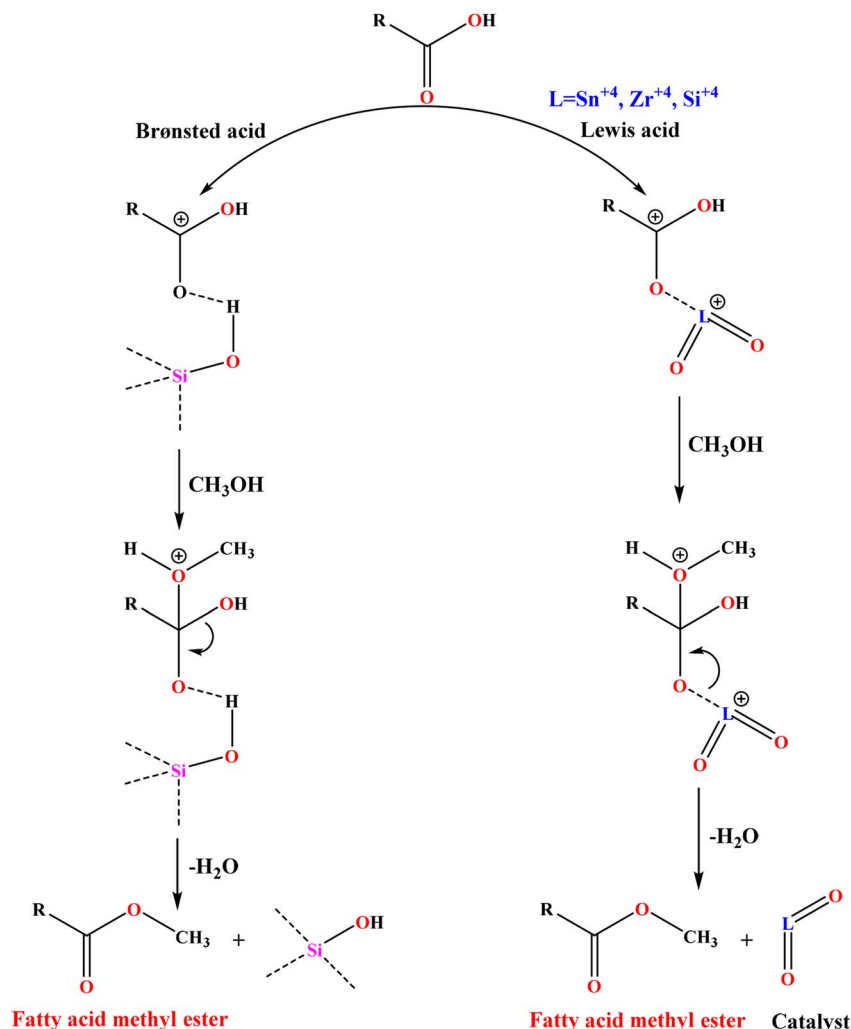


Fig. 5 Plausible mechanism of the esterification reaction using the Brønsted and Lewis acid sites of the SnZrSi oxide catalyst. Ref. 71, reprinted with permission of copyright© (2022) from Elsevier.

oil with methyl acetate. Yuan *et al.*⁷⁴ revealed that a ZnO/SnO₂@halloysite heterojunction photocatalyst prepared from zinc oxide and tin dioxide impregnated on layered kaolin could transesterify castor oil to biodiesel. The ZnO/SnO₂@H catalyst achieved a maximum biodiesel yield of 96.75%, and a yield of above 85% was maintained over five cycles. Furthermore, kinetic analysis showed quasi-first-order kinetics, with an activation energy of 75.02 kJ mol⁻¹. Lastly, the biodiesel produced could be prepared into B20 biodiesel to meet the EN 14214 and ASTM D6751 standards.

A TPA-impregnated SnO₂@Co-ZIF catalyst was prepared by Sahar and co-workers⁷⁵ and used in Mazari palm oil transesterification. The results showed that the TPA/SnO₂@Co-ZIF catalyst could achieve a high biodiesel yield of 94.05%, which is due to the presence of acid sites of different strengths. Additionally, a TPA-impregnated SnO₂@Mn-ZIF core-shell support was synthesized. It was reported that TPA/SnO₂@Mn-ZIF with 30 wt% TPA onto the support achieved a maximum biodiesel yield of 91.5%. After eight cycles, the yield reduced to about 30%.⁷⁶ Cui *et al.*⁷⁹ also developed rGO@SnO₂/ZnO

nanocomposites for biodiesel production from waste frying oil by the electrolysis approach. They reported that the rGO@SnO₂/ZnO nanocatalyst had a high specific area and appropriate functional groups. The biodiesel yield was 96.47% under optimized parameters, and after six reuse cycles, it reached 88.36%, indicating that the rGO@SnO₂/ZnO nanocatalyst has potential for sustainable and cost-effective industrial applications. Table 6 presents the works on biodiesel synthesis using tin oxide-based catalysts. Based on the acquired findings, tin oxide-based catalysts have been successfully applied as solid catalysts owing to their dual valency and ability to attain more than one oxidation state. However, the lower catalyst activity of tin oxide-based catalysts has also been observed. To improve the performance of tin oxide-based catalysts, strengthening the interaction between tin oxide and other acidic species in the solid catalyst is expected to enhance the catalyst activity and stability.

3.2.5 Iron oxide-based catalysts. Currently, iron oxide-based catalysts have been studied for biodiesel generation due to their desirable activity and magnetic properties, and the



Table 6 Comprehensive list of tin oxide-based catalysts for the biodiesel production process^a

Entry	Feedstock + alcohol	Catalyst	Characterizations	Conditions (time, temp., catalyst loading, molar ratio (acid (oil) : alcohol))	Yield (Y%/)/ conversion (C/%)	Reusability (run: C/Y)	Ref.
1	Stearic acid + methanol	SnZr _n	SA = 59.24, PV = 0.104, PD = 3.5, CA = 0.065	1 h, 120 °C, 0.2%, 1 : 150	Y = 74	7 runs: 68.8	70
2	Palmitic acid + methanol	SnO ₂ /ZrSiO ₄	SA = 66.19, PV = 0.062, PD = 1.87, CA = 0.214	2 h, 80 °C, 5%, 4 g : 85.6 mL	Y = 90.2	5 runs: 86.2	71
3	Bitter apple seed oil + methanol	Fe/SnO	N.R.	2 h, 50 °C, 1%, 1 : 10	Y = 98.1	N.R.	72
4	Rapeseed oil + methyl acetate	SnO@γ-Al ₂ O ₃	SA = 173, PV = 0.307, PD = 7.5	0.5 h, 210 °C, 10%, 1 : 40	Y = 33.5	3 runs: 18	73
5	Castor oil + methanol	ZnO/SnO ₂ @H	SA = 49.33, PV = 0.07, PD = 5.4	2 h, 75 °C, 4%, 1 : 12	Y = 96.8	5 runs: 86.1	74
6	Mazari palm oil + methanol	TPA/SnO ₂ @Co-ZIF	SA = 1281, PV = 0.51, PD = 1.83, CA = 6.437, CB = 6.861	3 h, 100 °C, 5%, 1 : 18	Y = 94.05	8 runs: >30	75
7	Mazari palm oil + methanol	TPA/SnO ₂ @Mn-ZIF	SA = 818, PV = 0.27, PD = 1.08, CA = 6.357, CB = 6.187	3 h, 100 °C, 6%, 1 : 18	Y = 91.5	8 runs: >30	76
8	Waste cooking oil + methanol	BTO@RGrO	SA = 9.64, PV = 0.056, PD = 12.87, CA = 3.884, CB = 2.9435	27.95 min, 68.83 °C, 3.21%, 1 : 14.93	C = 97.03	6 runs: 77.32	77
9	Soybean oil + methanol	MGO@SnO	N.R.	3 h, 120 °C, 5%, 1 : 10	Y = 96.5	8 runs: 64.6	78
10	Waste frying oil + methanol	rGO@SnO ₂ /ZnO	SA = 61.428, PV = 0.3178, PD = 21.46, CB = 0.20653	40 min, 65 °C, 3.5%, 1 : 12	Y = 96.47	7 runs: 88.36	79
11	Stearic acid + methanol	SnO ₂ -FA	SA = 11, PV = 0.0109, PD = 2.9, CB = 0.20653	1 h, 80 °C, 1.7%, 1 : 8	Y = 96.55	5 runs: 85.734	80

^a SA (surface area): m² g⁻¹; PV (pore volume): cm³ g⁻¹; PD (pore diameter): nm; CB (catalyst basicity): mmol g⁻¹; CA (catalyst acidity): mmol g⁻¹; not reported: N.R.; catalyst amount: relative to the weight of the oil feedstock; room temperature: RT.

catalytic performances of iron oxide-based catalysts are shown in Table 7. Elssawy *et al.*⁸¹ examined the iron oxide-based superacid catalyst (S₂/Fe₂O₃) for the esterification of oleic acid with methanol. This S₂/Fe₂O₃ catalyst was observed to be active in the esterification because it possessed good crystallinity, a mesoporous structure, effective intercalation of metal oxides with persulfate and graphene oxide, and high densities of

Brønsted and Lewis acid sites on the catalyst surface. Krishnan *et al.*⁸² produced oil palm empty fruit bunch-derived microcrystalline cellulose supported on γ-Fe₂O₃ magnetic acid catalysts, achieving a 92.1% yield in oleic acid esterification under ideal parameters. Meanwhile, the catalyst demonstrated rapid separation with reusability up to five cycles due to its ferromagnetic properties. In another study, Chutia *et al.*⁸⁴

Table 7 Comprehensive list of iron oxide-based catalysts for the biodiesel production process^a

Entry	Feedstock + alcohol	Catalyst	Characterizations	Conditions (time, temp., catalyst loading, molar ratio (acid (oil) : alcohol))	Yield (Y%/)/ conversion (C/%)	Reusability (run: C/Y)	Ref.
1	Oleic acid + methanol	S ₂ /Fe ₂ O ₃	SA = 44, PV = 0.32, PD = 11.5, CA = 0.8	3 h, 100 °C, 0.2 g, 1 : 5	Y = 96	6 runs: 80.3	81
2	Oleic acid + methanol	EFB-MCC/γ-Fe ₂ O ₃	SA = 290.55, PV = 0.249, PD = 3.5	2 h, 60 °C, 9%, 1 : 12	Y = 92.1	5 runs: 77.6	82
3	Schisandra chinensis seed oil + methanol	Fe ₃ O ₄ @SiO ₂ @ [C4mim]HSO ₄	SA = 10.1231, PV = 0.0169, PD = 6.6855	3 h, reflux, 1.5 g, 1 : 7	Y = 89.2	6 runs: 71.4	83
4	Mesua assamica oil + methanol	Fe ₃ O ₄ @biochar@SO ₃ H	SA = 71.47, PD = 87.4, CA = 3.9	80 min, 60 °C, 7%, 1 : 9	Y = 96.8	3 runs: 75.3	84
5	Palm oil + methanol	Fe ₃ O ₄ @SBA-15-NH ₂ -HPW	SA = 290.517, PV = 0.56, PD = 5.142	5 h, 150 °C, 4%, 1 : 20	Y = 91	6 runs: 80	85
6	Palm oil + methanol	CeO ₂ /ZSM-5@Fe ₃ O ₄	SA = 96.15, PV = 0.49, PD = 20.23, CA = 1.047, CB = 1.351	2.5 h, 25 °C, 3%, 1 : 18	Y = 95	4 runs: 79	86

^a SA (surface area): m² g⁻¹; PV (pore volume): cm³ g⁻¹; PD (pore diameter): nm; CB (catalyst basicity): mmol g⁻¹; CA (catalyst acidity): mmol g⁻¹; not reported: N.R.; catalyst amount: relative to the weight of the oil feedstock; room temperature: RT.





Fig. 6 Synthesis processes of the $\text{Fe}_3\text{O}_4@biochar@SO_3H$ nanocatalyst. Ref. 84, reprinted with permission of copyright© (2024) from Elsevier.

synthesized a magnetically separable $\text{Fe}_3\text{O}_4@biochar@SO_3H$ nanocatalyst from *Mesua assamica* waste seed shell biochar by the impregnation and sulfonation techniques (see Fig. 6) and employed it in the transesterification of different oil feedstock (*Mesua assamica* seed oil, *Jatropha* oil, and soybean oil) to produce biodiesel. The results illustrated that $\text{Fe}_3\text{O}_4@biochar@SO_3H$ possessed high acidity (3.9 mmol g^{-1}) and a high $-\text{SO}_3\text{H}$ density (1.8 mmol g^{-1}) for cost-effective biodiesel production. Moreover, the nanocatalyst achieved maximum yields of 96.8% *Mesua assamica* biodiesel, 95.3% *Jatropha* biodiesel, and 95.8% soybean biodiesel, respectively. Finally, the kinetic study of the transesterification reaction showed that a $32.42 \text{ kJ mol}^{-1}$ activation energy was required.

In another investigation, CeO_2 and Fe_3O_4 supported on ZSM-5 was synthesized by Liu *et al.*⁸⁶ and used for the biodiesel generation through the transesterification of palm oil under electrolytic assistance. Catalyst characterization confirmed that the abundant catalytically active sites in $\text{CeO}_2/\text{ZSM-5}@Fe_3O_4$ were attained due to the coral-like structure, and an approximately 95% biodiesel yield was obtained under the reaction

parameters. However, the $\text{CeO}_2/\text{ZSM-5}@Fe_3O_4$ catalyst appeared to show a drop in its activity after four cycles to 79%. Recently, Soares *et al.*⁸⁷ employed an $\alpha\text{-Fe}_2\text{O}_3$ film decorated with Pt nanoparticles for biodiesel production by the photoelectrochemical route, achieving a higher yield of biodiesel. Overall, iron oxide-based catalysts have exhibited high potential for biodiesel generation. Moreover, integration with support materials or composite structures is an effective strategy for enhancing the stability and reducing the agglomeration of iron oxide particles.

3.2.6 Aluminum oxide-based catalysts. Owing to their abundant acid sites, good structural and thermal stability, and high surface area, aluminum oxide-based catalysts have gained growing interest as supports/catalysts in many catalytic processes, such as biodiesel production, catalytic CO_2 methanation, and absorption. The catalytic performance of aluminum oxide-based catalysts is shown in Table 8. Munir *et al.*⁸⁸ explored the use of high oil-yielding *Quercus incana* seeds for synthesizing an Al_2O_3 nanocatalyst and used it in biodiesel production from inedible *Quercus incana* seed oil. This study achieved high

Table 8 Comprehensive list of aluminum oxide-based catalysts for the biodiesel production process^a

Entry	Feedstock + alcohol	Catalyst	Characterizations	Conditions (time, temp., catalyst loading, molar ratio (acid (oil) : alcohol))	Yield (Y%/)/ conversion (C%)	Reusability (run: C/Y)	Ref.
1	<i>Quercus incana</i> seed oil + methanol	Al_2O_3	N.R.	2 h, 70 °C, 0.25%, 1 : 9	Y = 97.6	5 runs: 93.6	88
2	Oleic acid + methanol	$\text{ZrO}_2/\text{Al}_2\text{O}_3$	CA = 0.635	12 h, 70 °C, 4%, 1 : 10	C = 90.5	4 runs: >80	89
3	Palm oil + methanol	$\text{La}_2\text{O}_3\text{-Al}_2\text{O}_3$	SA = 76.3, PV = 0.36, PD = 19.37, CA = 0.229, CB = 0.082	5 h, 200 °C, 5%, 1 : 30	Y = 93.12	1 run: 64.81	90
4	Oats lipid + methanol	$\text{CuO-ZnO-Al}_2\text{O}_3$	SA = 50.8, PV = 0.11, CA = 0.98	—, 70 °C, —, —	C = 97.6	5 runs: 93.8	91
5	Wet microbial biomass + ethanol	$\text{H}_3\text{PMo/Al}_2\text{O}_3$	N.R.	6 h, 200 °C, 15%, 1 : 120	C = 96.6	N.R.	92
6	Waste cooking oil + methanol	$\text{KNO}_3\text{-}\gamma\text{-Al}_2\text{O}_3$	SA = 46.93, PV = 0.18, PD = 9.01, CA = 2.1, CB = 2.9	3 h, 65 °C, 6%, 1 : 18	Y = 88.97	N.R.	93

^a SA (surface area): $\text{m}^2 \text{g}^{-1}$; PV (pore volume): $\text{cm}^3 \text{g}^{-1}$; PD (pore diameter): nm; CB (catalyst basicity): mmol g^{-1} ; CA (catalyst acidity): mmol g^{-1} ; not reported: N.R.; catalyst amount: relative to the weight of the oil feedstock; room temperature: RT.



oil conversion yields in the presence of Al_2O_3 , and no significant loss of activity was observed after five consecutive reuses. Alkahlawy *et al.*⁸⁹ developed $\text{ZrO}_2/\text{Al}_2\text{O}_3$ catalysts by a sol-gel technique and further evaluated their catalytic activity for biodiesel synthesis from oleic acid. The authors claimed that the used $\text{ZrO}_2/\text{Al}_2\text{O}_3$ catalyst was promising and showed a 90.5% conversion of biodiesel. In another similar study, a bifunctional acid-base $\text{La}_2\text{O}_3\text{-Al}_2\text{O}_3$ catalyst was synthesized by Kingkam *et al.*;⁹⁰ the authors claimed that new weak basic sites with appropriate acid site amounts were attained at an La_2O_3 loading of 40% and a calcination temperature of 600 °C, and the catalyst achieved a yield of 93.2% under ideal conditions. Surprisingly, the $\text{La}_2\text{O}_3\text{-Al}_2\text{O}_3$ catalyst appeared to show an obvious drop in its activity after the first run to 64.81%; this was due to the leaching of La^{3+} ions during the reaction process.

Recently, Bento and co-workers⁹² reported $\text{H}_3\text{PMo}/\text{Al}_2\text{O}_3$ and used it as a heterogeneous acid catalyst for the simultaneous esterification and transesterification of lipid-rich fungal biomass. A maximum biodiesel conversion of about 96.6% was attained. Suresh *et al.*⁹³ synthesized carbon from oil palm leaves incorporated into $\text{KNO}_3/\gamma\text{-Al}_2\text{O}_3$, and it was further used as a catalyst in the methanolysis of waste cooking oil for the production of biodiesel. Catalyst characterization confirmed that $\text{KNO}_3\text{-C}/\gamma\text{-Al}_2\text{O}_3$ had K_2O , K_2O_2 , and K_2C_2 species on its surface and possessed high total basicity and acidity. More importantly, the biodiesel produced met the fuel property requirements outlined in ASTM D6751 and EN 14214 standards. All of these studies demonstrate that aluminum oxide-based materials are effective solid catalysts.

3.2.7 Titania-based catalysts. Among various metal oxides, titania (TiO_2) is preferred because of its low cost, high specific surface area, and abundant acid sites, and it shows better and stronger interactions with other active components. Bekhradnassab and co-workers⁹⁵ reported a 3D cheese-like Mn-doped TiO_2 catalyst for the esterification of oleic acid. Experimental results showed that the selected Mn(4)Ti(MW) catalyst exhibited an 89.1% conversion within 4 h, and the oleic acid conversion

reduced by only 1% after six cycles. In another similar study, Hou *et al.*⁹⁷ fabricated hierarchical porous Mo/Ce/H- TiO_2 catalysts through an evaporation-induced self-assembly method. Catalyst characterizations confirmed that the dual Mo/Ce oxides with Brønsted-Lewis acidic sites were finely supported on the TiO_2 support and could act as active centers for catalyzing the transesterification-esterification of low-value acidic oils. They achieved a 93.8% oil conversion within 8 h using the Mo/Ce/H- TiO_2 catalyst. Interestingly, the better FFA and water-tolerant capacity were also found for Mo/Ce/H- TiO_2 catalysts.

Sulfonated $\text{TiO}_2\text{-GO}$ core-shell solid spheres were synthesized by a two-step hydrothermal microwave-assisted method. This catalyst possessed desirable textural properties and strong acidity and was employed for the conversion of palm fatty acid distillate to biodiesel (see Fig. 7). As a result, the biodiesel yield was 96.7% under ideal conditions. After 10 cycles, the biodiesel yield reached 72.49%, and the reduction in the biodiesel yield was ascribed to the leaching of the sulfate into the reaction mixture and the deposition of organic compounds on mesoporous channels.⁹⁸ Sabzevar *et al.*⁹⁹ studied the esterification of oleic acid to biodiesel employing the TiO_2 -decorated magnetic ZIF-8 nanocatalyst ($\text{Fe}_3\text{O}_4@\text{ZIF-8}/\text{TiO}_2$). The various characterization results revealed that the $\text{Fe}_3\text{O}_4@\text{ZIF-8}/\text{TiO}_2$ catalyst was well-formed. This catalyst exhibited oleic acid conversions up to 80% and 93% using ethanol and methanol under optimum conditions, respectively. A summary of titania-based catalysts for producing biodiesel is presented in Table 9. These studies demonstrate that titania-based catalysts are promising for the production of industrially viable biodiesel.

3.2.8 Zirconium-based catalysts. The suitable surface area and medium acidic sites of zirconium allow its use as a catalyst or a catalyst support for biodiesel synthesis. Quite interestingly, the surface hydroxyl groups or unsaturated Zr species of zirconium-based catalysts can serve as acid sites. Table 10 exhibits the zirconium-based catalysts used in the biodiesel production process. Yusuf *et al.*¹⁰¹ investigated the transesterification reaction of soybean oil to biodiesel employing

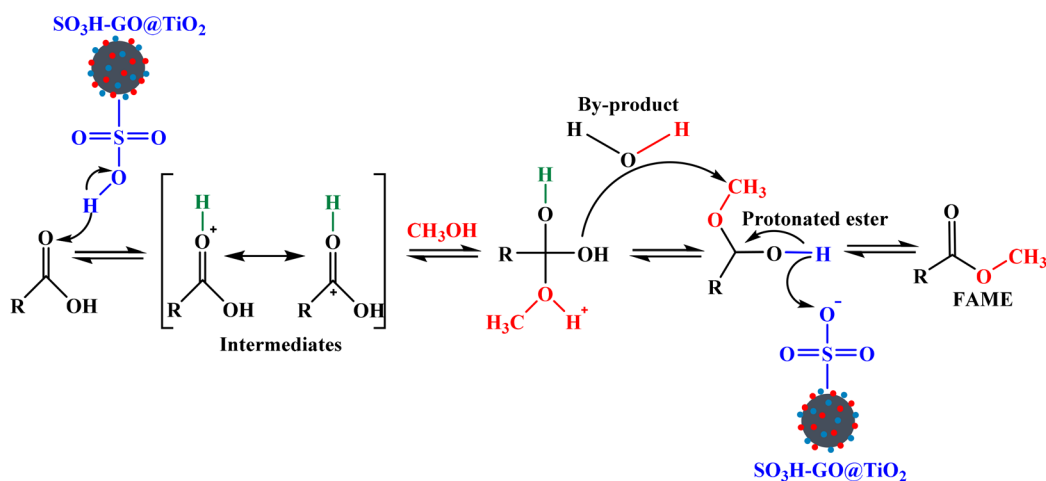


Fig. 7 Scheme of the proposed mechanism for the esterification by the mesoporous $\text{SO}_3\text{H-GO@TiO}_2$ catalyst. Ref. 98, reprinted with permission of copyright© (2021) from Elsevier.



Table 9 Comprehensive list of titania-based catalysts for the biodiesel production process^a

Entry	Feedstock + alcohol	Catalyst	Characterizations	Conditions (time, temp., catalyst loading, molar ratio (acid (oil) : alcohol))	Yield (Y%/conversion (C%/))	Reusability (run: C/Y)	Ref.
1	Oleic acid + methanol	TiO ₂ (UVA)	SA = 51.851, PV = 0.74, PD = 3.52	4 h, 55 °C, 20%, 1 : 55	Y = 98	5 runs: 71	94
2	Oleic acid + methanol	Mn(4) Ti(MW)	SA = 68.7, PV = 0.058, CA = 42.777	4 h, 110 °C, 9%, 1 : 20	C = 89.1	6 runs: 88	95
3	Waste oil + methanol	MnFeTi (ILS)	SA = 1.3143, PV = 0.002947, PD = 50, CA = 1.057	1.5 h, 110 °C, 9%, 1 : 20	C = 91.43	6 runs: 85.44	96
4	Low-value acidic oils + methanol	Mo/Ce/H-TiO ₂	SA = 329.35, PV = 0.35, PD = 7.22, CA = 0.647	8 h, 140 °C, 5%, 1 : 30	C = 93.8	5 runs: 82.1	97
5	Palm fatty acid distillate + methanol	SO ₃ H-GO@TiO ₂	SA = 611, PV = 0.16, PD = 7.25, CA = 3.3	40 min, 70 °C, 3%, 1 : 9	Y = 96.7	10 runs: 72.49	98
6	Oleic acid + ethanol	Fe ₃ O ₄ @ZIF-8/TiO ₂	N.R.	62.5 min, 50 °C, 6%, 1 : 30	Y = 80.04	5 runs: 77.22	99
7	Palmitic acid + methanol	0.5TMS5	SA = 219, PV = 0.23, PD = 3.14, CA = 0.985	4.5 h, RT, 3%, 1 : 20	C = 95.9	3 runs: >95	100

^a SA (surface area): m² g⁻¹; PV (pore volume): cm³ g⁻¹; PD (pore diameter): nm; CB (catalyst basicity): mmol g⁻¹; CA (catalyst acidity): mmol g⁻¹; not reported: N.R.; catalyst amount: relative to the weight of the oil feedstock; room temperature: RT.

a zeolite-supported ZrO₂ catalyst (ZrO₂/ZSM-5) and a series of desilicated ZrO₂/ZSM-5 catalysts. As a result, the desilication process of the zeolite could enhance the mesoporous volume and external surface area without destroying the crystallinity or microporosity of the catalysts. The as-prepared ZrO₂/ZSM-5(0.2 M) catalyst exhibited a conversion of 97.84% biodiesel because the desilicated catalyst demonstrated better activity than ZrO₂/ZSM-5. This high conversion was attributed to the high number of active sites and high dispersion of ZrO₂ on the desilicated ZSM-5 with improved acidity. Asif *et al.*¹⁰² synthesized a bi-functional Sr/ZrO₂ catalyst for biodiesel synthesis from chicken fat oil. As a result, 7% Sr/ZrO₂ was found to achieve a significantly higher conversion than three naturally occurring bi-functional catalysts (zwitterions). Ghasemi *et al.*¹⁰³ used a bifunctional CaO-ZrO₂ nanocatalyst for the esterification and transesterification of waste cooking oil. The results obtained showed that the Zr-Ca/kaolin(T)-U(300) catalyst exhibited high activity for producing biodiesel with total conversion, FFA conversion, and TG conversion rates of 93.4%, 99.0%, and 73.4%, respectively. After five cycles, the conversion reached

91.3%, implying that the structure and crystallinity of the nanocatalyst had excellent stability. Based on the literature, it is also noted that a high surface-area zirconium support might therefore be an important factor for catalytic reactivity. Thus, several new methods should be explored for the synthesis of zirconium-based materials with high surface areas.

3.3 Mixed metal oxide-based catalysts

Mixed metal oxides are formed by the conjunction of two or more metal oxides, and these composites combine the beneficial properties of both components can promote the esterification and transesterification processes for biodiesel generation. Pasupulety *et al.*¹⁰⁴ synthesized mesoporous tantalum-zirconium mixed oxide (TZ) by the sol-gel method for the esterification and transesterification of soybean oil containing higher water and FFA contents. As a result, the yields of methyl palmitate (95.0%) and soybean oil biodiesel (88.6%) at 180 °C using the TZ catalyst were higher than those with ZrO₂ alone. The high activity of this catalyst was associated with

Table 10 Comprehensive list of zirconium-based catalysts for the biodiesel production process^a

Entry	Feedstock + alcohol	Catalyst	Characterizations	Conditions (time, temp., catalyst loading, molar ratio (acid (oil) : alcohol))	Yield (Y%/conversion (C%/))	Reusability (run: C/Y)	Ref.
1	Soybean oil + methanol	ZrO ₂ /ZSM-5(0.2 M)	SA = 387.32, PV = 0.29, PD = 4.63	4 h, 200 °C, 1%, 1 : 16	C = 97.84	3 runs: 93.8	101
2	Chicken fat oil + methanol	7% Sr/ZrO ₂	SA = 119.8, PV = 0.2154, PD = 8.21	20 min, 70 °C, 1%, 1 : 14	C = 75	N.R.	102
3	Waste cooking oil + methanol	Bifunctional CaO-ZrO ₂	SA = 22.49, PV = 0.09, CA = 0.453, CB = 0.324	3 h, 110 °C, 10%, 1 : 20	C = 93.4	5 runs: 91.3	103

^a SA (surface area): m² g⁻¹; PV (pore volume): cm³ g⁻¹; PD (pore diameter): nm; CB (catalyst basicity): mmol g⁻¹; CA (catalyst acidity): mmol g⁻¹; not reported: N.R.; catalyst amount: relative to the weight of the oil feedstock; room temperature: RT.



enhanced acidity because of the existence of Ta–O–Ta, Ta=O, and Zr–O–Ta species. More importantly, 80.0% yellow grease biodiesel generation was attained on the TZ catalyst at 180 °C. In another study, Cr–Al mixed oxide was modified with different amounts of 12-tungstophosphoric acid (TPA) and employed in the biodiesel production from low-cost wild olive oil. This catalyst showed a 93% biodiesel yield under ideal conditions, and after five times of reuse, its yield showed no substantial loss. Furthermore, the biodiesel produced exhibited the same characteristics as the conventional petrodiesel.¹⁰⁸

In recent years, Li *et al.*¹¹¹ synthesized a mesoporous SrTiO₃ perovskite catalyst by the sol–gel method with high tolerance for FFAs and moisture. Additionally, this catalyst was evaluated for the transesterification of palm oil with methanol. The highest biodiesel yield of 93.14% was attained under ideal conditions. Interestingly, biodiesel yields of 83.8% and 86.5% were obtained even with the oleic acid and water addition of 10 wt% and 5 wt%, respectively. Furthermore, the molecular simulation results showed that the Sr active sites tended to be retained, which is attributed to the protection of the Ti sites during the reaction process. Similarly, magnetic CoFe₂O₄ and MnFe₂O₄ nanoparticles coated with sulfonated lignin were prepared from sugarcane bagasse lignin employing acetyl sulfate and used as acid catalysts for the esterification of oleic acid. It was observed that a maximum oleic acid conversion of approximately 80%

was obtained by the prepared magnetic catalysts.¹¹² Silva Junior *et al.*¹¹³ also synthesized copper molybdate nanoplates (Cu₃(MoO₄)₂(OH)₂). It was observed that the Cu₃(MoO₄)₂(OH)₂ catalyst showed nanometer sizes with a surface area of 70.77 m² g⁻¹. Additionally, the authors claimed that the used nanoplates were promising and showed a 98.38% conversion of oleic acid.

Naushad *et al.*¹¹⁶ prepared two catalysts ([NiFe₂O₄@BMSI]Br and [NiFe₂O₄@BMSI]HSO₄) *via* the ion-exchange process (see Fig. 8), characterized their catalytic properties, and further evaluated their catalytic efficacy for the transesterification of vegetable oil. The results revealed that [NiFe₂O₄@BMSI]HSO₄ exhibited better performance than [NiFe₂O₄@BMSI]Br. A yield of 86.4% was attained using [NiFe₂O₄@BMSI]HSO₄, while in the case of [NiFe₂O₄@BMSI]Br, it was about 74.6%. More references for the immobilization of acidic functional groups on mixed metal oxides (Zn_{0.4}Ni_{0.6}Fe₂O₄@SO₃H,¹¹⁷ CoFe₂O₄@SGO,¹¹⁸ and AlFe₂O₄@n-Pr@Et-SO₃H¹¹⁹) for biodiesel generation were also studied.

Ibrahim *et al.*¹²⁰ synthesized the CoFe₂O₄@MoS₂ magnetic acid catalyst with a strong saturation magnetization of 15.78 emu g⁻¹ *via* the sol–gel method and employed it in the esterification of oleic acid by the microwave-assisted method. The conversion of oleic acid reached 98.2% using CoFe₂O₄@MoS₂. This catalyst showed stable catalytic activity for up to eight uses, with a conversion of oleic acid of 98.2%. Table 11 shows the

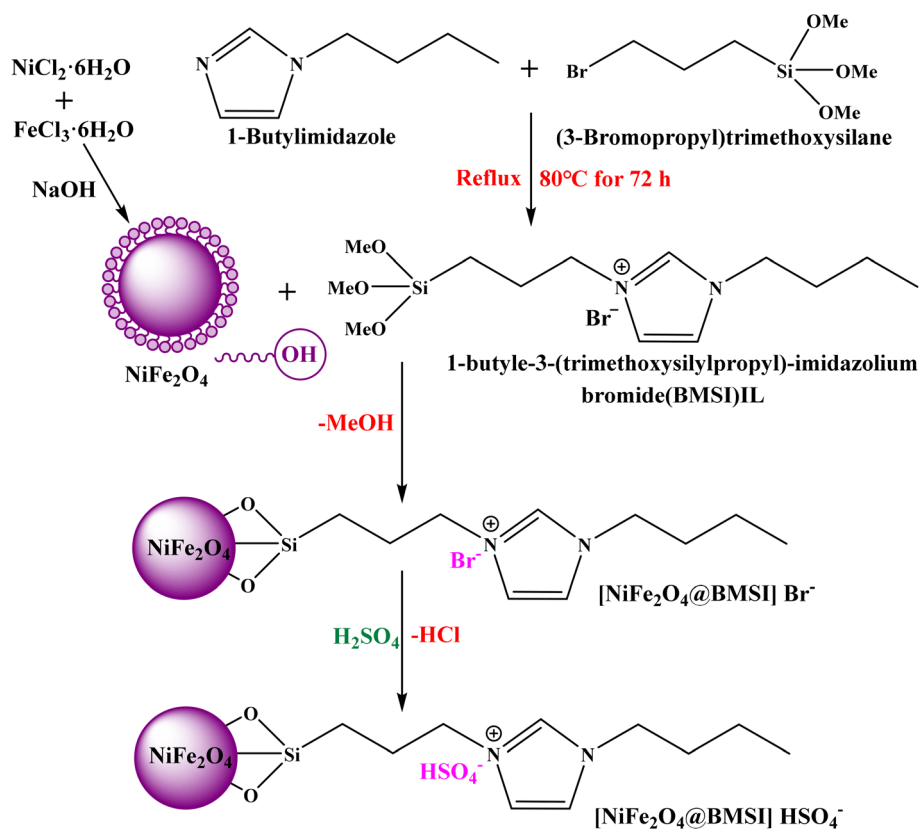


Fig. 8 Preparation methods for [NiFe₂O₄@BMSI]Br and [NiFe₂O₄@BMSI]HSO₄. Ref. 116, reprinted with permission of copyright© (2021) from Elsevier.



Table 11 Comprehensive list of mixed metal oxide-based catalysts for the biodiesel production process^a

Entry	Feedstock + alcohol	Catalyst	Characterizations	Conditions (time, temp., catalyst loading, molar ratio (acid (oil) : alcohol))	Yield (Y%)/conversion (C%)	Reusability (run: C/Y)	Ref.
1	Soybean oil + methanol	20TZ	SA = 162, PV = 0.221, CA = 0.38	4 h, 180 °C, 3%, 1 : 20	Y = 88.6	3 runs: 67	104
2	Waste cooking oil + methanol	Si-Zn oxide	SA = 0.41, PV = 0.0091, PD = 13.306, CA = 0.367, CB = 0.402	3 h, 150 °C, 3%, 1 : 15	Y = 91.99	5 runs: 87.39	105
3	Waste cooking oil + methanol	V ₂ O ₅ -CaO	SA = 6.3, PV = 0.0085, CA = 8.5191, CB = 11.1835	3 h, 60 °C, 1%, 1 : 20	Y = 78.48	N.R.	106
4	Mustard oil + methanol	NiO-CdO-Nd ₂ O ₃	N.R.	5 h, 80 °C, 0.5 g, 1 : 15	Y = 80	3 runs: >70	107
5	Wild olive oil + methanol	TPA/Cr-Al	SA = 56.168, PV = 0.014, PD = 1.5085	5 h, 80 °C, 4%, 1 : 21	Y = 93	5 runs: without any substantial loss	108
6	Waste cooking oil + methanol	SiO-ZnO/MOF	SA = 2.18, PV = 0.0096, PD = 3.78, CA = 0.02, CB = 2.84	5 min (microwave), 80 °C, 5%, 1 : 11	Y = 99.5	3 runs: >94.3	109
7	Oleic acid + ethanol	Fe ₂ (MoO ₄) ₃	N.R.	5 h, 70 °C, 3%, 1 : 9	C = 90.5	6 runs: 87.5	110
8	Palm oil + methanol	SiTiO ₃ -SG	SA = 13.07, PV = 0.096, CA = 0.078, CB = 0.15	3 h, 170 °C, 6%, 1 : 15	Y = 93.14	3 runs: 85.68	111
9	Oleic acid + methanol	CoFe ₂ O ₄ -SL5	SA = 41.47, PV = 0.1219, PD = 9.25	6 h, 100 °C, 5%, 1 : 10	Y = 79.2	N.R.	112
10	Oleic acid + methanol	Cu ₃ (MoO ₄) ₂ (OH) ₂	SA = 70.77	5 h, 140 °C, 5%, 1 : 5	C = 98.38	7 runs: 85.66	113
11	Oleic acid + methanol	ZnMoO ₄	SA = 0.37, CA = 0.181	2 h, 160 °C, 3%, 1 : 12	C = 88	N.R.	114
12	Acidified oil + methanol	SiZr _{0.75} Fe _{0.25} O ₃	SA = 4.5, PD = 8.9, CA = 20.0, CB = 44.4	3.4 h, 178 °C, 4.5%, 1 : 19	Y = 99.5	5 runs: 96.2	115
13	Palm oil + methanol	[NiFe ₂ O ₄ @BMS][HSO ₄]	SA = 87.21	8 h, 80 °C, 5%, 1 : 12	Y = 86.4	6 runs: 92.7 (catalytic activity)	116
14	<i>Salicornia Persica Akhani</i> oil + methanol	Zn _{0.4} Ni _{0.6} Fe ₂ O ₄ @SO ₃ H	CA = 2.5 (mmol SO ₃ H per g)	4 h, 60 °C, 1.59%, 1 : 5	Y = 96	5 runs: 85.7	117
15	Waste coconut scum oil + methanol	CoFe ₂ O ₄ @SGO	SA = 106.25, PV = 0.033, PD = 12.73	33.08 min, 64.73 °C, 2.24%, 1 : 12.41	Y = 96.87	6 runs: 90.17	118
16	Oleic acid + methanol	AlFe ₂ O ₄ @n-Pr@Et-SO ₃ H	N.R.	2 h, 60 °C, 0.04 g, 1 : 4	Y = 98	5 runs: 94	119
17	Oleic acid + methanol	CoFe ₂ O ₄ @MoS ₂	SA = 6.7, CA = 2.1	2 h, 140 °C, 7.5%, 1 : 15	C = 98.2	8 runs: 87.2	120
18	Waste coconut scum oil + methanol	SnFe ₂ O ₄ /cigarette butt-derived biochar	SA = 128.47, PV = 0.276, PD = 15.62, CB = 1.048	34.25 min, 64.05 °C, 2.73%, 1 : 11.81	Y = 98.67	7 runs: 90.48	121
19	Waste cooking oil + methanol	ZnFe ₂ O ₄ (5)/CaO _{PS}	SA = 1.63, PD = 22.13, CA = 1.804	212.22 min, 63.69 °C, 5.06%, 1 : 12.96	Y = 96.89	5 runs: <80	122

^a SA (surface area): m² g⁻¹; PV (pore volume): cm³ g⁻¹; PD (pore diameter): nm; CB (catalyst basicity): mmol g⁻¹; CA (catalyst acidity): mmol g⁻¹; not reported: N.R.; catalyst amount: relative to the weight of the oil feedstock; room temperature: RT.



works on biodiesel production under different conditions using mixed metal oxide-based catalysts. As shown in the table, the mixed metal oxides utilized in catalyst formulation play a pivotal role in determining key physicochemical properties, such as surface acidity and basicity, surface area, and magnetic properties, which are critical parameters influencing the catalytic reactivity. Thus, additional investigations are still required to determine catalyst formulations, develop a simple synthesis process, and enhance the interaction in the composites of various metal oxides.

3.4 MOF-derived metal oxide-based catalysts

Recently, metal–organic frameworks (MOFs) have exhibited intrinsic characteristics, such as augmented surface areas, high porosities, and tunable functionalities.^{123,124} In addition, MOFs can eliminate the non-stable linker and generate porous metal oxide materials using various strategies (*e.g.*, thermal decomposition, chemical treatment, reflux synthesis, and electrochemical synthesis), promoting their diverse applications.^{125,126} MOF-derived metal oxides benefit from their inherited morphology and controllable dimension, making them a promising heterogeneous catalyst candidate.¹²⁷ So far, several researchers have reported studies on the application of MOF-derived metal oxide-based catalysts for biodiesel production. Yang *et al.*¹²⁸ reported that the Zn-based MOF-derived MgO@ZnO hybrids are excellent nanocatalysts for biodiesel production from soybean oil. Ruatpuia and co-workers¹²⁹ designed a ZIF-8 MOF-derived CaO/ZnO nanocatalyst for the high-yielding transesterification of soybean oil to biodiesel. Lu and co-workers¹³⁰ developed flower-like mesoporous sulfated zirconia nanosheets (SZNs) through the thermal decomposition of *in situ* sulfated Zr-MOFs. Due to their large surface area (186.1 m² g⁻¹) and the strong bonding between sulfate and zirconia atoms, the acid performance tests revealed that SZNs have good catalytic activity and reusability for the transesterification. Apart from that, Wang *et al.*¹³¹ utilized bimetallic CaFe-MOF derivatives in the transesterification of palm oil and methanol. The characterization results clearly demonstrated that CaO and Ca₂Fe₂O₅ are the major active sites in the CaFe-MOF derivatives. Meanwhile, CaFe-800-1 showed good activity, and the conversion of 98.53% was achieved. Furthermore, the obtained biodiesel product satisfied the standards of ASTM D6751 and EN 14214. Recently, our group also studied the generation of biodiesel from FFAs with methanol over heteropolyacids incorporated into single/bimetallic MOF derivatives (*e.g.*, PW-TiO₂, HSiW@ZrO₂-300, HSiW@Ni-Zr-O and HPW@Ni-Zr-O). All these composite catalysts exhibited excellent catalytic performance and reusability, and the FFA conversion of 95.2% was obtained under optimal reaction conditions.^{132–135} However, based on the literature studies, the preparation of MOF-derived catalysts is extremely expensive.¹³⁶ Moreover, some MOF-derived metal oxides are still unstable in the reaction system, which potentially results in the pore collapse of the original MOF structure.¹³⁷ Thus, designing and developing a cost-effective strategy for the fabrication of MOF-derived single metal oxide and mixed metal oxide heterogeneous acid catalysts

with unique morphologies, stable structures, and excellent catalytic performance are significant research targets for the future.

4. Conclusions and outlook

In the present review, the use of various metal oxides as heterogeneous acid catalysts for biodiesel production using esterification/transesterification reactions has been examined. This includes a comprehensive examination of the properties, preparation methods, and catalytic applications of sulfated metal oxide catalysts, metal oxide-based acid catalysts (they were classified into eight types: silica-based catalysts, molybdenum oxide-based catalysts, tungsten oxide-based catalysts, tin oxide-based catalysts, iron oxide-based catalysts, aluminum oxide-based catalysts, titania-based catalysts, and zirconium-based catalysts), mixed metal oxide-based acid catalysts, and MOF-derived metal oxide-based catalysts. We note that metal oxide heterogeneous acid catalysts are examples of heterogeneous catalysts, which are in demand in order to address the inherent problems of homogeneous acid catalysts. Moreover, metal oxides when combined with active substances, such as metal nanoparticles, heteropolyacid, loaded functional groups, zeolite, ionic liquids, and lipases, can result in increased surface area and active sites and improved catalytic performance during reactions. However, their practical application is hindered by challenges related to the following aspects:

(1) The preparation processes of metal oxide heterogeneous acid catalysts are generally complex and lengthy, which restricts large-scale utilization. Thus, different simple and low-cost methods for metal oxide heterogeneous acid catalyst preparation should be encouraged and investigated.

(2) For catalyst development, improving the stability of metal oxide heterogeneous acid catalysts is one of the key focuses. Therefore, novel preparation techniques (*e.g.*, microwave, ultrasonic, and plasma techniques) and surface modifications (*e.g.*, doping with various metal ions, constructing enzyme-chemical synergistic catalytic interface structures, and introducing oxygen and other defect structures, hydrophobic structures, active site nanoclusters or single-atomization) may prevent the leaching and degradation of active species and improve the resilience of metal oxides, ensuring their scalability and long-term cycling stability in biodiesel synthesis.

(3) Based on previous research, the structure–performance relationship of metal oxide-based heterogeneous acid composite catalysts remains uncertain. Consequently, substantial efforts should be made to understand the real structure–capacity relationship and its synergistic effects under diverse operating conditions, and this aspect may be assisted by computational methods.

(4) Although the strong acidity of sulfated metal oxides is gaining increasing research attention, the leaching of sulfate groups during the reaction is the most important drawback. Thus, a detailed investigation on the nature of the active sulfate groups and the mechanism of their formation should be performed.



(5) Also, the combination of metal oxides with porous frameworks, polymers, or nanomaterial substrates to create multifunctional composite catalysts may increase the active sites and facilitate sustainable biodiesel generation.

(6) Based on the literature, the use of MOF-derived metal oxide-based composites as acid catalysts for biodiesel production is rarely reported. Thus, the design and fabrication of efficient and durable MOF-derived metal oxide-based acid catalysts with specific morphologies and structures (e.g., core-shell structure, hierarchical structure, 3D porous structure, hollow structure, and nanofiber structure) are required to drive the future development of MOF-derived functional heterogeneous catalysts. Meanwhile, combining the exciting features of MOF-derived metal oxide and artificial intelligence (AI) technologies would promote the development of commercial-scale biofuel production.

(7) The application of metal oxide heterogeneous acid catalysts in the production process of biodiesel are in the form of powder, which may be challenging to manage. This result may cause potential secondary pollution. Future research can explore modifying the shape of catalysts, constructing films, or combining them with magnetic materials to enhance the management and recycling of catalysts.

The utilization of metal oxide heterogeneous acid catalysts in large-scale industrial biodiesel production is still under development. However, through continuous innovation in the high-performance material design, preparation process optimization, and practical implementation, metal oxide heterogeneous acid catalysts can be transformed into efficient and scalable solutions for more sustainable and economically competitive biodiesel production.

Author contributions

Qiuyun Zhang: investigation, validation, writing – original draft, writing – review and editing, and project administration; Jialu Wang: investigation, visualization; Xiaojuan Zhang: writing – review and editing; Taoli Deng: visualization, writing – review and editing; Yutao Zhang: writing – review and editing, supervision, and funding acquisition; Peihua Ma: validation, writing – review and editing.

Conflicts of interest

The authors declare that they have no known competing financial interests or personal relationships that could have appeared to influence the work reported in this paper.

Data availability

No primary research results, software or code have been included and no new data were generated or analyzed as part of this review.

Acknowledgements

This work was financially supported by the National Natural Science Foundation of China (22262001), the Porous Materials and Green Catalysis Innovation Team in High Education Institute of Guizhou Province (Qianjiaoji[2023]086), the Key Laboratory of Agricultural Resources and Environment in High Education Institute of Guizhou Province (Qianjiaoji[2023]025), the Key Laboratory of Bioenergy Conversion and Green Materials in Anshun University (asxykpt202502), and the 2018 Thousand Level Innovative Talents Training Program of Guizhou Province.

References

- 1 J. Y. Kim, D. Kwon, J. H. Yim, Y. Kim, Y. J. Jeon and E. E. Kwon, Sustainable biodiesel synthesis via non-catalytic transesterification of biomass waste-derived oil and ethanol, *Green Chem.*, 2025, DOI: [10.1039/D5GC02712H](https://doi.org/10.1039/D5GC02712H).
- 2 H. Li, T. Wang, D. Guo, N. Bingwa, Y. Xu, R. Liu, Q. Xiao, G. Li, Y. Wang, H. Yu and X. Ma, A robust microwave-absorbing solid alkaline catalyst synthesis via CaSr-BTC for green and efficient biodiesel production, *Chem. Eng. J.*, 2025, **507**, 160771.
- 3 A. A. Tigro, S. M. Hailegiorgis and A. S. Reshad, Heterogeneous alkaline calcium oxide nano-catalyst supported on porous materials for the transesterification reaction: A review, *Results Eng.*, 2025, **27**, 105912.
- 4 T. G. Desta, G. G. Gebresilasie, G. G. Meressa, S. K. Abraha, M. W. Weldeslassie, K. Y. Abdu, Y. A. Endris and M. A. Shah, Production and characterization of biodiesel from *Jatropha curcas* seed oil by using fly ash as a catalyst, *ACS Omega*, 2025, **10**, 25498–25505.
- 5 Q. Zhang, Y. Lei, J. Wang, Y. Zhang and P. Ma, Zeolitic imidazolate frameworks-based materials for accelerating sustainable biodiesel production: A mini review, *Catal. Surv. Asia*, 2025, **29**(195), 214.
- 6 B. Rezki, Y. Essamlali, O. Amadine, S. Sair, M. Aadila and M. Zahouily, Microwave-driven oleic acid esterification over chlorosulfonic acid-treated hydroxyapatite: synergism for intensified biodiesel production, *RSC Adv.*, 2024, **14**, 33019–33033.
- 7 M. S. Abishek and S. Kachhap, Sustainable synthesis of copper oxide nanoparticles using *Spondias mombin* and biodiesel production from *Guizotia abyssinica*: Engine performance, emission characteristics, and machine learning-based optimization, *Fuel*, 2025, **392**, 134804.
- 8 Q. Y. Zhang, M. Deng, X. X. Li, N. Xu, T. Li, Q. Liu, Z. J. Liu and Y. T. Zhang, Different ligand functionalized Al-based MOFs as a support for impregnation of heteropoly acid for efficient esterification reactions, *Appl. Organomet. Chem.*, 2025, **39**, e70217.
- 9 B. Panchal, C. H. Su, C. C. Fu, S. J. Wu and H. Y. Juan, Ecofriendly and cost-effective biodiesel production from water containing feedstocks through electrolysis-A review, *Fuel Process. Technol.*, 2025, **276**, 108277.



- 10 O. A. Mawlid, H. H. Abdelhady and M. S. El-Deab, Recent advances in magnetic nanoparticle-based heterogeneous catalysts for efficient biodiesel production: A review, *Energy Fuels*, 2024, **38**, 20169–20195.
- 11 C. H. Su, Recoverable and reusable hydrochloric acid used as a homogeneous catalyst for biodiesel production, *Appl. Energy*, 2013, **104**, 503–509.
- 12 H. Helmiyati, J. V. Hapsari, R. Bakri, I. Abdullah, A. Umar and D. O. B. Apriandanu, Nanocellulose-coated magnetite-strontium oxide as novel green catalyst for biodiesel production from waste cooking oil: Optimization using RSM, *Fuel*, 2025, **396**, 135236.
- 13 Q. Zhang, Y. Wu, X. Hong, Z. Li, Y. Lei, R. Yu, T. Deng, Y. Zhang and P. Ma, Different ligand functionalized bimetallic (Zr/Ce)UiO-66 as a support for immobilization of phosphotungstic acid with enhanced activity for the esterification of fatty acids, *Sustainable Chem. Pharm.*, 2024, **37**, 101344.
- 14 H. Zhou, L. Dai, D. Liu and W. Du, MOF-derived hierarchically ordered porous carbon for the immobilization of Eversa® Transform 2.0 and its post-immobilization hydrophobization in biodiesel production, *Fuel*, 2023, **339**, 127426.
- 15 Q. Y. Zhang, X. Y. Hong, J. Lei, Y. T. Lei, Y. G. Yang, J. S. Cheng, Y. L. Hu and Y. T. Zhang, Environmentally-friendly preparation of Sn(II)-BDC supported heteropolyacid as a stable and highly efficient catalyst for esterification reaction, *J. Saudi Chem. Soc.*, 2024, **28**, 101832.
- 16 H. Ghaedrahmat, M. Y. Masoomi and M. Zendeהל, Synthesize and characterization of ZIF-8/NaP zeolite composites as a stable acid-base catalyst for organic reactions, *Polyhedron*, 2023, **236**, 116372.
- 17 Q. Zhang, T. Li, Z. Li, Y. Lei, X. Hong, M. Deng, J. Cheng, Z. Liu and Y. Zhang, Facile synthesis of silver-exchanged phosphotungstic acid immobilized on Sn-Bi bimetallic metal-organic frameworks for enhanced esterification, *Appl. Organomet. Chem.*, 2025, **39**, e7799.
- 18 A. M. Rozina, T. C. Ezeji, O. Emmanuel, N. Qureshi and A. Khan, Utilization of waste seed oil from *Cestrum nocturnum* as a novel source for cleaner production of biodiesel using green nano-catalyst of antimony oxide, *Fuel*, 2024, **364**, 131124.
- 19 S. Kumar, S. Kumari, A. Kumari, J. Ahmed, R. Jasrotia, A. Kandwal and R. Sharma, Sustainable and green production of biodiesel from *Calotropis procera* seed oil using CuO nanocatalyst, *J. Inorg. Organomet. Polym. Mater.*, 2024, **34**, 3258–3269.
- 20 N. C. Joshi, P. Gururani, P. Bhatnagar, V. Kumar and M. S. Vlaskin, Advances in metal oxide-based nanocatalysts for biodiesel production: A review, *ChemBioEng Rev.*, 2023, **10**, 258–271.
- 21 O. Awogbemi, A. A. Ojo and S. A. Adeleye, Advancements in the application of metal oxide nanocatalysts for sustainable biodiesel production, *Discover Appl. Sci.*, 2024, **6**, 250.
- 22 J. Liu, S. Niu, Y. Xu, S. Liu, J. Zhu, Z. Yang, J. Geng, Y. Zhang and Y. Hao, Sustainable biodiesel production using acid-base bifunction supported catalysts, *Biomass Bioenergy*, 2025, **200**, 108032.
- 23 H. S. Siow, K. Sudesh, P. Murugan and S. Ganesan, Mealworm (*Tenebrio molitor*) oil characterization and optimization of the free fatty acid pretreatment via acid-catalyzed esterification, *Fuel*, 2021, **299**, 120905.
- 24 J. M. Encinar, S. Nogales-Delgado and N. Sánchez, Pre-esterification of high acidity animal fats to produce biodiesel: A kinetic study, *Arabian J. Chem.*, 2021, **14**, 103048.
- 25 S. Lüneburger, A. L. Gallina, L. C. Soares and D. M. Benvegnú, Biodiesel production from *Hevea Brasiliensis* seed oil, *Fuel*, 2022, **324**, 124639.
- 26 M. Supeno, J. P. Sihotang, Y. V. Panjaitan, D. S. Y. Damanik, J. Br. Tarigan and E. K. Sitepu, Room temperature esterification of high-free fatty acid feedstock into biodiesel, *RSC Adv.*, 2023, **13**, 33107–33113.
- 27 R. Estrada, K. Alon-alon, J. Simbajon, J. Pañares, E. Pagalan, A. Ido and R. Arazo, Reduction of acid value of waste cooking oil through optimized esterification via central composite design, *Circ. Econ. Sustainability*, 2024, **4**, 1819–1834.
- 28 I. Istadi, D. D. Anggoro, L. Buchori, D. A. Rahmawati and D. Intaningrum, Active acid catalyst of sulphated zinc oxide for transesterification of soybean oil with methanol to biodiesel, *Procedia Environ. Sci.*, 2015, **23**, 385–393.
- 29 M. N. Hossain, M. S. U. S. Bhuyan, A. H. M. A. Alam and Y. C. Seo, Biodiesel from hydrolyzedwaste cooking oil using a S-ZrO₂/SBA-15 super acid catalyst under sub-critical conditions, *Energies*, 2018, **11**, 299.
- 30 A. Aneu, K. Wijaya and A. Syoufian, Porous silica modification with sulfuric acids and potassium fluorides as catalysts for biodiesel conversion from waste cooking oils, *J. Porous Mater.*, 2022, **29**, 1321–1335.
- 31 M. Utami, R. Safitri, M. F. Pradipta, K. Wijaya, S. W. Chang, B. Ravindran, D. Ovi, J. R. Rajabathar, N. Poudineh and R. M. Gengan, Enhanced catalytic conversion of palm oil into biofuels by Cr-incorporated sulphated zirconia, *Mater. Lett.*, 2022, **309**, 131472.
- 32 B. O. Yusuf, S. A. Oladepo and S. A. Ganiyu, Biodiesel production from waste cooking oil via β -zeolite-supported sulfated metal oxide catalyst systems, *ACS Omega*, 2023, **8**, 23720–23732.
- 33 M. A. Hassan, W. Wang, B. Dong, H. Anwar, Z. Chang, D. Wei and K. Khan, Production of biodiesel from waste culinary oil catalyzed by S₂O₈²⁻/TiO₂-SiO₂ solid super-acid catalyst prepared with recovered TiO₂ from spent SCR, *Mater. Today Sustainability*, 2024, **26**, 100730.
- 34 K. Föttinger, E. Halwax and H. Vinek, Deactivation and regeneration of Pt containing sulfated zirconia and sulfated zirconia, *Appl. Catal., A*, 2006, **301**, 115–122.
- 35 X. Chen, Q. Zhang, S. Li, H. Wang, X. Zhang, L. Chen, L. Ma and J. Liu, The efficient promoting hydrodeoxygenation of bioderived furans over Pd/HPW-SiO₂ by phosphotungstic acid, *Fuel Process. Technol.*, 2024, **258**, 108095.
- 36 B. Changmai, A. E. H. Wheatley, R. Rano, G. Halder, M. Selvaraj, U. Rashid and S. L. Rokhum, A magnetically



- separable acid-functionalized nanocatalyst for biodiesel production, *Fuel*, 2021, **305**, 121576.
- 37 A. F. Peixoto, M. M. A. Soliman, T. V. Pinto, S. M. Silva, P. Costa, E. C. B. A. Alegria and C. Freire, Highly active organosulfonic aryl-silica nanoparticles as efficient catalysts for biomass derived biodiesel and fuel additives, *Biomass Bioenergy*, 2021, **145**, 105936.
- 38 V. Hegde, P. Pandit, P. Rananaware and V. P. Brahmkhatri, Sulfonic acid-functionalized mesoporous silica catalyst with different morphology for biodiesel production, *Front. Chem. Sci. Eng.*, 2022, **16**, 1198–1210.
- 39 M. Y. Saleh, A. K. O. Aldulaimi, S. M. Saeed and A. H. Adha, $\text{TiFe}_2\text{O}_4@\text{SiO}_2\text{-SO}_3\text{H}$: A novel and effective catalyst for esterification reaction, *Heliyon*, 2024, **10**, e26286.
- 40 Q. Shu, X. Liu, Y. Huo, Y. Tan, C. Zhang and L. Zou, Construction of a Brønsted-Lewis solid acid catalyst $\text{La-PW-SiO}_2/\text{SWCNTs}$ based on electron withdrawing effect of La(III) on π bond of SWCNTs for biodiesel synthesis from esterification of oleic acid and methanol, *Chin. J. Chem. Eng.*, 2022, **44**, 351–362.
- 41 B. Ghasemzadeh, A. A. Matin, B. Habibi and M. Ebadi, $\text{Cotton/Fe}_3\text{O}_4@\text{SiO}_2@\text{H}_3\text{PW}_{12}\text{O}_{40}$ a magnetic heterogeneous catalyst for biodiesel production: Process optimization through response surface methodology, *Ind. Crops Prod.*, 2022, **181**, 114806.
- 42 M. F. Paiva, G. A. A. Diab, E. S. D. T. de Mendonça, S. C. L. Dias and J. A. Dias, Synthesis, characterization, and application of phosphotungstic acid supported on iron-based magnetic nanoparticles coated with silica, *Catal. Today*, 2022, **394–396**, 425–433.
- 43 J. Ding, C. Zhou, Z. Wu, C. Chen, N. Feng, L. Wang, H. Wan and G. Guan, Core-shell magnetic nanomaterial grafted spongy-structured poly (ionic liquid): A recyclable brønsted acid catalyst for biodiesel production, *Appl. Catal., A*, 2021, **616**, 118080.
- 44 P. Mohammadpour and E. Safaei, Biodiesel and adipic acid production using molybdenum(VI) complex of a bis(phenol) diamine ligand supported on Fe_3O_4 magnetic nanoparticles, *Fuel*, 2022, **327**, 124831.
- 45 D. Xue, Y. Jiang and F. Zheng, Magnetic-responsive solid acid catalysts for esterification, *RSC Adv.*, 2023, **13**, 27579–27588.
- 46 I. Fatimah, G. Purwiantono, I. Sahroni, S. Sagadevan, W. Chun-Oh, S. A. I. S. M. Ghazali and R. Doong, Recyclable catalyst of ZnO/SiO_2 prepared from *Salacca leaves* ash for sustainable biodiesel conversion, *S. Afr. J. Chem. Eng.*, 2022, **40**, 134–143.
- 47 N. H. Embong, N. Hindryawati, P. Bhuyar, N. Govindan, M. H. A. Rahim and G. P. Maniam, Enhanced biodiesel production via esterification of palm fatty acid distillate (PFAD) using rice husk ash (NiSO_4)/ SiO_2 catalyst, *Appl. Nanosci.*, 2023, **13**, 2241–2249.
- 48 M. Y. Albalushi, G. Abdulkreem-Alsultan, N. Asikin-Mijan, M. I. bin Saiman, Y. P. Tan and Y. H. Taufiq-Yap, Efficient and stable rice husk biderived silica supported $\text{Cu}_2\text{S-FeS}$ for one pot esterification and transesterification of a malaysian palm fatty acid distillate, *Catalysts*, 2022, **12**, 1537.
- 49 K. Li and W. L. Xie, Enhanced biodiesel production from low-value acidic oils using ordered hierarchical macroporous MoAl@H-SiO_2 catalyst, *Fuel*, 2024, **364**, 131105.
- 50 G. S. M. Leão, M. D. S. Ribeiro, R. L. de Freitas Filho, L. B. Saraiva, R. R. Peña-García, A. P. de Carvalho Teixeira, R. M. Lago, F. A. Freitas, S. de Sá Barros, S. D. Junior, Y. L. Ruiz and F. X. Nobre, The synergic effect of h-MoO_3 , $\alpha\text{-MoO}_3$, and $\beta\text{-MoO}_3$ phase mixture as a solid catalyst to obtain methyl oleate, *ACS Appl. Mater. Interfaces*, 2024, **16**, 60103–60121.
- 51 A. M. Sabzevar and M. Ghahramaninezhad, Development of an impressive method for the synthesis of $\alpha\text{-MoO}_3$ nanobelts as an efficient catalyst for biodiesel production, *Environ. Sci. Pollut. Res.*, 2024, **31**, 65273–65287.
- 52 B. Chaudhry, M. Ahmad, M. Munir, M. F. Ramadan, M. Munir, C. U. Mussagy, S. Faisal, T. M. M. Abdellatif and A. Mustafa, Unleashing the power of non-edible oil seeds of *Ipomoea cairica* for cleaner and sustainable biodiesel production using green molybdenum oxide (MoO_3) nano catalyst, *Sustainable Energy Technol. Assess.*, 2024, **65**, 103781.
- 53 Q. Wang, W. L. Xie and L. H. Guo, Molybdenum and zirconium oxides supported on KIT-6 silica: A recyclable composite catalyst for one-pot biodiesel production from simulated low-quality oils, *Renewable Energy*, 2022, **187**, 907–922.
- 54 X. Gao, C. Chen, W. Zhang, Y. Hong, C. Wang and G. Wu, Sulfated TiO_2 supported molybdenum-based catalysts for transesterification of *Jatropha* seed oil: Effect of molybdenum species and acidity properties, *Renewable Energy*, 2022, **191**, 357–369.
- 55 V. L. de Brito, M. A. Gonçalves, H. C. L. dos Santos, G. N. da Rocha Filho and L. R. V. da Conceição, Biodiesel production from waste frying oil using molybdenum over niobia as heterogeneous acid catalyst: Process optimization and kinetics study, *Renewable Energy*, 2023, **215**, 118947.
- 56 M. Majedi and E. Safaei, Molybdenum (VI) complex of resorcinol-based ligand immobilized on silica-coated magnetic nanoparticles for biodiesel production, *Appl. Organomet. Chem.*, 2023, **37**, e7216.
- 57 P. M. M. da Silva, M. A. Gonçalves, A. P. da Luz Corrêa, P. T. S. da Luz, J. R. Zamian, G. N. da Rocha Filho and L. R. V. da Conceição, Preparation and characterization of a novel efficient catalyst based on molybdenum oxide supported over graphene oxide for biodiesel synthesis, *Renewable Energy*, 2023, **211**, 126–139.
- 58 W. Zhang, C. Wang, B. Luo, P. He, L. Li and G. Wu, Biodiesel production by transesterification of waste cooking oil in the presence of graphitic carbon nitride supported molybdenum catalyst, *Fuel*, 2023, **332**, 126309.
- 59 W. Zhang, C. Wang, B. Luo, P. He, L. Zhang and G. Wu, Efficient and economic transesterification of waste cooking soybean oil to biodiesel catalyzed by outer



- surface of ZSM-22 supported different Mo catalyst, *Biomass Bioenergy*, 2022, **167**, 106646.
- 60 J. S. B. Figueiredo, B. T. S. Alves, V. A. Freire, J. J. N. Alves and B. V. S. Barbosa, Preparation, characterization and evaluation of x-MoO₃/Al-SBA-15 catalysts for biodiesel production, *Mater. Renewable Sustainable Energy*, 2022, **11**, 17–31.
- 61 J. C. F. Cavalcante, A. M. da Silva, P. M. B. Caldas, B. V. de Sousa Barbosa, H. B. da Silva Júnior and J. J. N. Alves, Characterization and optimization of biodiesel production from corn oil using heterogeneous MoO₃/MCM-41 catalysts, *Catal. Today*, 2025, **446**, 115119.
- 62 J. S. B. Figueiredo, N. E. Souza, B. T. S. Alves, A. M. Silva, B. V. S. Barbosa, N. R. C. Huaman, R. R. Menezes and J. J. N. Alves, MoO₃ catalyst supported on micro-mesoporous structure for biodiesel production, *Catal. Lett.*, 2025, **155**, 52.
- 63 V. Gunasekaran, H. Gurusamy, G. Ravi and Y. Rathinam, Sustainable synthesis of bio-diesel and jet-fuel range hydrocarbons from poisonous Abrus Precatorius seed oil over MoO₃-HPW/Ga-KIT-6, *Renewable Energy*, 2024, **224**, 120130.
- 64 M. A. Gonçalves, E. K. L. Mares, J. R. Zamian, G. N. da Rocha Filho and L. R. V. da Conceição, Statistical optimization of biodiesel production from waste cooking oil using magnetic acid heterogeneous catalyst MoO₃/SrFe₂O₄, *Fuel*, 2021, **304**, 121463.
- 65 M. A. Gonçalves, H. C. L. dos Santos, M. A. R. da Silva, A. da Cas Viegas, G. N. da Rocha Filho and L. R. V. da Conceição, Biodiesel production from waste cooking oil using an innovative magnetic solid acid catalyst based on Ni-Fe ferrite: RSM-BBD optimization approach, *J. Ind. Eng. Chem.*, 2024, **135**, 270–285.
- 66 N. Mansir, S. H. Teo, N. A. Mijan and Y. H. Taufiq-Yap, Efficient reaction for biodiesel manufacturing using bifunctional oxide catalyst, *Catal. Commun.*, 2021, **149**, 106201.
- 67 H. C. L. dos Santos, M. A. Gonçalves, A. da Cas Viegas, B. A. M. Figueira, P. T. S. da Luz, G. N. da Rocha Filho and L. R. V. da Conceição, Tungsten oxide supported on copper ferrite: a novel magnetic acid heterogeneous catalyst for biodiesel production from low quality feedstock, *RSC Adv.*, 2022, **12**, 34614–34626.
- 68 V. C. dos Santos-Durndell, L. J. Durndell, M. A. Isaacs, A. F. Lee and K. Wilson, WO_x/ZrO_x functionalised periodic mesoporous organosilicas as water-tolerant catalysts for carboxylic acid esterification, *Sustainable Energy Fuels*, 2023, **7**, 1677–1686.
- 69 C. Y. Hsu, Z. H. Mahmoud, N. Kamolova, K. Muzammil, F. H. Alsultany, S. H. Z. Al-Abdeen and E. Kianfar, Photosynthesis of polypyrrole/ZnFe₂O₄-WO₃ nanocomposite for biodiesel production, *Fuel Process. Technol.*, 2025, **271**, 108193.
- 70 S. M. Ibrahim, Preparation, characterization and application of novel surface modified ZrSnO₄ as Sn-based TMOs catalysts for the stearic acid esterification with methanol to biodiesel, *Renewable Energy*, 2021, **173**, 151–163.
- 71 S. M. Ibrahim and A. Mustafa, Synthesis and characterization of new bifunctional SnZrSi oxide catalysts for biodiesel production, *J. Mol. Liq.*, 2022, **354**, 118811.
- 72 M. Hanif, I. A. Bhatti, M. Zahid and M. Shahid, Production of biodiesel from non-edible feedstocks using environment friendly nano-magnetic Fe/SnO catalyst, *Sci. Rep.*, 2022, **12**, 16705.
- 73 C. Prestigiacomo, M. Biondo, A. Galia, E. Monflier, A. Ponchel, D. Prevost, O. Scialdone, S. Tilloy and R. Bleta, Interesterification of triglycerides with methyl acetate for biodiesel production using a cyclodextrin-derived SnO@γ-Al₂O₃ composite as heterogeneous catalyst, *Fuel*, 2022, **321**, 124026.
- 74 Z. Yuan, J. Zhu, J. Lu, Y. Li and J. Ding, Preparation of biodiesel by transesterification of castor oil catalyzed by flaky halloysite supported ZnO/SnO₂ heterojunction photocatalyst, *Renewable Energy*, 2024, **227**, 120516.
- 75 J. Sahar, M. Farooq, A. Ramli, A. Naeem, N. S. Khattak and Z. A. Ghazi, Highly efficient heteropoly acid decorated SnO₂@Co-ZIF nanocatalyst for sustainable biodiesel production from Nannorrhops ritchiana seeds oil, *Renewable Energy*, 2022, **198**, 306–318.
- 76 J. Sahar, M. Farooq, A. Ramli, A. Naeem and N. S. Khattak, Biodiesel production from Mazari palm (Nannorrhops ritchiana) seeds oil using tungstophosphoric acid decorated SnO₂@Mn-ZIF bifunctional heterogeneous catalyst, *Appl. Catal., A*, 2022, **643**, 118740.
- 77 M. Safaripour, M. Saidi and H. R. Nodeh, Synthesis and application of barium tin oxide-reduced graphene oxide nanocomposite as a highly stable heterogeneous catalyst for the biodiesel production, *Renewable Energy*, 2023, **217**, 119199.
- 78 L. Peng, A. Bahadoran, S. Sheidaei, P. J. Ahranjani, H. Kamyab, B. Oryani, S. S. Arain and S. Rezaia, Magnetic graphene oxide supported tin oxide (SnO) nanocomposite as a heterogeneous catalyst for biodiesel production from soybean oil, *Renewable Energy*, 2024, **224**, 120050.
- 79 P. Cui, C. Gao, L. Gu, Z. Li and B. Liao, rGO@SnO₂/ZnO nanocomposite as a highly reactive heterogeneous catalyst toward biodiesel synthesis by electrolysis procedure: Central composite design optimization, *Process Saf. Environ. Prot.*, 2024, **191**, 287–303.
- 80 R. Chakraborty, S. K. Das, A. Sarkar and K. Sondhi, Environmental impact assessment of sustainable methyl stearate (biodiesel) synthesis employing fly ash supported tin oxide catalyst, *Cleaner Chem. Eng.*, 2022, **4**, 100077.
- 81 A. A. Elssawy, M. M. T. El-Tahawy and H. A. Khalaf, Green synthesis of iron oxide-based superacid catalysts modified with graphene oxide for efficient esterification reactions, *Catal. Surv. Asia*, 2025, **29**, 111–126.
- 82 S. G. Krishnan, F. L. Pua and F. Zhang, Oil palm empty fruit bunch derived microcrystalline cellulose supported magnetic acid catalyst for esterification reaction: An



- optimization study, *Energy Convers. Manage.: X*, 2022, **13**, 100159.
- 83 J. Yu, Y. Wang, L. Sun, Z. Xu, Y. Du, H. Sun, W. Li, S. Luo, C. Ma and S. Liu, Catalysis preparation of biodiesel from waste schisandra chinensis seed oil with the ionic liquid immobilized in a magnetic catalyst: $\text{Fe}_3\text{O}_4@\text{SiO}_2@[\text{C4mim}]\text{HSO}_4$, *ACS Omega*, 2021, **6**, 7896–7909.
- 84 G. P. Chutia and K. Phukan, Facile synthesis of $\text{Fe}_3\text{O}_4@\text{biochar}@\text{SO}_3\text{H}$ as magnetically separable Bronsted acid nanocatalyst for biodiesel production from different oil feedstocks, *Ind. Crops Prod.*, 2024, **215**, 118578.
- 85 P. Zhang, P. Liu, M. Fan, P. Jiang and A. Haryono, High-performance magnetite nanoparticles catalyst for biodiesel production: Immobilization of 12-tungstophosphoric acid on SBA-15 works effectively, *Renewable Energy*, 2021, **175**, 244–252.
- 86 S. Liu, S. Niu, H. Yu, K. Han, S. Xia, Z. Yang, Y. Zheng, Y. Zhang, Y. Hao and A. Abulizi, Electrolysis combined with magnetic $\text{CeO}_2/\text{ZSM-5}@\text{Fe}_3\text{O}_4$ catalyst to boost transesterification for biodiesel production, *Fuel*, 2024, **378**, 132862.
- 87 W. N. Soares, A. G. R. Costa, R. M. P. Silva, S. G. Lima, T. P. Braga, I. Costa, Jr G. E. Luz and R. S. Santos, Biodiesel photoelectrocatalytic synthesis employing $\alpha\text{-Fe}_2\text{O}_3$ film decorated with Pt nanoparticles as photoanode, *Catal. Today*, 2025, **444**, 114997.
- 88 M. Munir, M. Ahmad, A. A. Alsahli, L. Zhang, S. Islamov, S. Sultana, C. U. Mussagy, A. Mustafa, M. Munir, B. Chaudhry, M. Hamayun and S. Khawaja, Harnessing non-edible *Quercus incana* seeds for sustainable and clean biodiesel production using seed-derived green Al_2O_3 nanocatalyst, *Sustainable Energy Technol. Assess.*, 2024, **72**, 104025.
- 89 A. Alkahlawy and A. Gaffer, Novel sustainable biodiesel production from low-grade oleic acid via esterification catalyzed by characterized crystalline $\text{ZrO}_2/\text{Al}_2\text{O}_3$, *BMC Chem.*, 2025, **19**, 5.
- 90 W. Kingkam, S. Nuchdang, C. Phalakornkule, U. Suwanmanee and D. Rattanaphra, Synergistic effect of $\text{La}_2\text{O}_3\text{-Al}_2\text{O}_3$ based catalysts for efficient biodiesel production, *J. Ind. Eng. Chem.*, 2025, **143**, 197–212.
- 91 V. N. Nandini Devi, N. Padmamalini and A. Asha, Production of high calorific biodiesel from oats lipid using $\text{Cu-ZnO-Al}_2\text{O}_3$ Catalyst, *Catal. Lett.*, 2025, **155**, 57.
- 92 H. B. S. Bento, C. E. R. Reis, P. G. Cunha, A. K. F. Carvalho and H. F. De, One-pot fungal biomass-to-biodiesel process: Influence of the molar ratio and the concentration of acid heterogenous catalyst on reaction yield and costs, *Fuel*, 2021, **300**, 120968.
- 93 J. Suresh, H. S. Yong, N. B. Talib, J. Matmin, N. I. W. Azelee, S. J. M. Rosid and S. Toemen, Biomass-incorporated $\text{KNO}_3\text{-C}/\gamma\text{-Al}_2\text{O}_3$ bifunctional catalyst for efficient biodiesel production, *Renewable Energy*, 2024, **234**, 121239.
- 94 R. A. Welter, H. Santana, L. G. de la Torre, M. Robertson, O. P. Taranto and M. Oelgemöller, Methyl oleate synthesis by TiO_2 photocatalytic esterification of oleic acid: Optimisation by response surface quadratic methodology, reaction kinetics and thermodynamics, *ChemPhotoChem*, 2022, **6**, e202200007.
- 95 E. Bekhradinassab, A. Tavakoli, M. Haghghi and M. Shabani, Catalytic biofuel production over 3D macrostructured cheese-like Mn-promoted TiO_2 isotype: Mn-catalyzed microwave-combustion design, *Energy Convers. Manage.*, 2022, **251**, 114916.
- 96 E. Bekhradinassab, A. Tavakoli, M. Haghghi and M. Shabani, 2-hydroxyethylammoniumsulfate ionic liquid performance as simultaneous fuel and sulfating agent in tablet-like manganese and iron incorporated titania synthesis: Biodiesel production from waste oil, *Fuel*, 2023, **340**, 127402.
- 97 S. X. Hou and W. L. Xie, Three-dimensional hierarchical meso/macroporous Mo/Ce/TiO_2 composites enhances biodiesel production from acidic soybean oil by transesterification-esterifications, *Energy Convers. Manage.*, 2024, **305**, 118273.
- 98 S. Soltani, N. Khanian, T. S. Y. Choong, N. Asim and Y. Zhao, Microwave-assisted hydrothermal synthesis of sulfonated $\text{TiO}_2\text{-GO}$ core-shell solid spheres as heterogeneous esterification mesoporous catalyst for biodiesel production, *Energy Convers. Manage.*, 2021, **238**, 114165.
- 99 A. M. Sabzevar, M. Ghahramaninezhad and M. N. Shahrak, Enhanced biodiesel production from oleic acid using TiO_2 -decorated magnetic ZIF-8 nanocomposite catalyst and its utilization for used frying oil conversion to valuable product, *Fuel*, 2021, **288**, 119586.
- 100 D. Guliani, A. Sobti and A. P. Toor, Titania impregnated mesoporous MCM-48 as a solid photo-catalyst for the synthesis of methyl palmitate: Reaction mechanism and kinetics, *Renewable Energy*, 2022, **191**, 405–417.
- 101 B. O. Yusuf, S. A. Oladepo and S. A. Ganiyu, Zr-modified desilicated ZSM-5 catalysts as highly active and recyclable catalysts for production of biodiesel from soybean oil: Insight into improved catalyst properties, acidity and dispersion through desilication, *Fuel*, 2023, **351**, 128729.
- 102 M. Asif, F. Javed, M. Younas, M. A. Gillani, W. B. Zimmerman and F. Rehman, Investigating biodiesel production from Chicken fat oil using bi-functional catalysts and microbubble mediated mass transfer, *Fuel*, 2024, **358**, 130125.
- 103 I. Ghasemi, M. Haghghi, E. Bekhradinassab and A. Ebrahimi, Ultrasound-assisted dispersion of bifunctional CaO-ZrO_2 nanocatalyst over acidified kaolin for production of biodiesel from waste cooking oil, *Renewable Energy*, 2024, **225**, 120287.
- 104 N. Pasupulety, A. A. Al-zahrani, M. A. Daous, H. Driss and H. Alhumade, Highly efficient tantalum-zirconium oxide catalysts for biodiesel production from higher water and FFA containing soybean oil or yellowgrease feedstocks, *Fuel*, 2022, **324**, 124513.
- 105 S. Liu, Z. Li, K. Han, Y. Wang, S. Niu, J. Liu, J. Zhu and Y. Zheng, Biodiesel production from waste cooking oil through transesterification catalyzed by the strontium-



- zinc bifunctional oxides, *Chem. Eng. Process.*, 2024, **200**, 109777.
- 106 M. Mulyatun, J. Prameswari, I. Istadi and W. Widayat, Synthesis method effect on the catalytic performance of acid-base bifunctional catalysts for converting low-quality waste cooking oil to biodiesel, *Catal. Lett.*, 2024, **154**, 4837–4855.
- 107 M. Zeeshan, S. Ghazanfar, M. Tariq, H. M. Asif, A. Hussain, M. Usman, M. A. Khan, K. Mahmood, M. Sirajuddin and M. Imran, Synthesis of novel ternary NiO-CdO-Nd₂O₃ nanocomposite for biodiesel production, *Renewable Energy*, 2023, **210**, 800–809.
- 108 I. M. G. Ul, M. T. Jan, M. Farooq, A. Naeem, I. W. Khan and H. U. Khattak, Biodiesel production from wild olive oil using TPA decorated Cr-Al acid heterogeneous catalyst, *Chem. Eng. Res. Des.*, 2022, **178**, 540–549.
- 109 J. Yang, W. J. Cong, Z. Y. Zhu, Z. D. Miao, Y. T. Wang, M. Nelles and Z. Fang, Microwave-assisted one-step production of biodiesel from waste cooking oil by magnetic bifunctional SrO-ZnO/MOF catalyst, *J. Cleaner Prod.*, 2023, **395**, 136182.
- 110 A. A. AlKahlaway, M. A. Betiha, D. Aman and A. M. Rabie, Facial synthesis of ferric molybdate (Fe₂(MoO₄)₃) nanoparticle and its efficiency for biodiesel synthesis via oleic acid esterification, *Environ. Technol. Innovation*, 2021, **22**, 101386.
- 111 Y. Li, S. Niu, J. Wang, W. Zhou, Y. Wang, K. Han and C. Lu, Mesoporous SrTiO₃ perovskite as a heterogeneous catalyst for biodiesel production: Experimental and DFT studies, *Renewable Energy*, 2022, **184**, 164–175.
- 112 L. H. R. Varão, T. A. L. Silva, H. D. Z. Zamora, L. C. de Moraes and D. Pasquini, Synthesis of methyl biodiesel by esterification using magnetic nanoparticles coated with sulfonated lignin, *Biomass Convers. Biorefin.*, 2023, **12**, 12277–12290.
- 113 J. L. Silva Junior, F. X. Nobre, F. A. de Freitas, T. A. F. de Carvalho, S. S. de Barros, M. C. Nascimento, L. Manzato, J. M. E. Matos, W. R. Brito, Y. Leyet and P. R. C. Couceiro, Copper molybdate synthesized by sonochemistry route at room temperature as an efficient solid catalyst for esterification of oleic acid, *Ultrason. Sonochem.*, 2021, **73**, 105541.
- 114 L. A. Colaço, A. S. Sousa, A. C. F. M. Costa, A. F. F. Farias and I. M. G. Santos, Zinc molybdate: A new catalyst for biodiesel synthesis by simultaneous esterification/transesterification reaction, *Fuel*, 2024, **371**, 132066.
- 115 Y. Zhang, S. Niu, S. Xia, S. Liu and J. Liu, One-step conversion of acidified oil to biodiesel by novel bifunctional SrZr_{1-x}Fe_xO₃ catalyst, *Renewable Energy*, 2023, **217**, 119139.
- 116 M. Naushad, T. Ahamad and M. R. Khan, Fabrication of magnetic nanoparticles supported ionic liquid catalyst for transesterification of vegetable oil to produce biodiesel, *J. Mol. Liq.*, 2021, **330**, 115648.
- 117 A. Karimian, S. H. Pourhoseini and A. Nozari, Persica Akhiani Salicornia as novel biodiesel feedstock production for economic prosperity in salty and water scarcity areas: Optimized oil extraction process and transesterification reaction using new magnetic heterogenous nanocatalysts, *Renewable Energy*, 2023, **211**, 361–369.
- 118 Q. Li, Y. Zhao, T. Liu, Z. Luo, K. Luo and T. Wang, Kinetic and optimization study of ultrasound-assisted biodiesel production from waste coconut scum oil using porous CoFe₂O₄@sulfonated graphene oxide magnetic nanocatalysts: CI engine approach, *Renewable Energy*, 2024, **236**, 121457.
- 119 D. Singh, K. Singh, Y. Jadeja, S. V. Menon, P. Singh, S. M. Ibrahim, M. Singh, M. K. Abosaoda, S. B. Al Reshaidan and M. A. El-Meligy, Magnetic nano-sized solid acid catalyst bearing sulfonic acid groups for biodiesel synthesis and oxidation of sulfides, *Sci. Rep.*, 2025, **15**, 1397.
- 120 A. S. I. Ibrahim, B. Gözmen and Ö. Sönmez, Esterification of oleic acid using CoFe₂O₄@MoS₂ solid acid catalyst under microwave irradiation, *Fuel*, 2024, **371**, 131988.
- 121 Y. Man, M. Habibi and B. Maleki, Biodiesel synthesis from waste coconut scum oil utilizing SnFe₂O₄/cigarette butt-derived biochar as a magnetic nanocatalyst: Optimization, kinetic and thermodynamic study, *Chem. Eng. Res. Des.*, 2024, **210**, 311–327.
- 122 H. Fu, Y. Xiao, A. Abulizi, K. Okitsu, Y. Maeda and T. Ren, Surfactant-modified ZnFe₂O₄/CaO_{PS} porous acid-base bifunctional catalysts for biodiesel production from waste cooking oil and process optimization, *J. Environ. Chem. Eng.*, 2024, **12**, 114234.
- 123 N. P. S. Chauhan, P. Perumal, N. S. Chundawat and S. Jadoun, Achiral and chiral metal-organic frameworks (MOFs) as an efficient catalyst for organic synthesis, *Coord. Chem. Rev.*, 2025, **533**, 216536.
- 124 Q. Zhang, T. Yang, X. Liu, C. Yue, L. Ao, T. Deng and Y. Zhang, Heteropoly acid-encapsulated metal-organic framework as a stable and highly efficient nanocatalyst for esterification reaction, *RSC Adv.*, 2019, **9**, 16357–16365.
- 125 H. Liu, M. Dong, J. Xiong, Z. Huang, H. Hou, Y. Liang and J. Lu, MOF-derived Ni-Co bimetallic catalyst facilitated the gasification of surface carbon during DRM process, *J. Environ. Chem. Eng.*, 2025, **13**, 116948.
- 126 P. Behera, S. Subudhi, S. P. Tripathy and K. Parida, MOF derived nano-materials: A recent progress in strategic fabrication, characterization and mechanistic insight towards divergent photocatalytic applications, *Coord. Chem. Rev.*, 2022, **456**, 214392.
- 127 J. Chen, R. Abazari, K. A. Adegoke, N. W. Maxakato, O. S. Bello, M. Tahir, S. Tasleem, S. Sanati, A. M. Kirillov and Y. Zhou, Metal-organic frameworks and derived materials as photocatalysts for water splitting and carbon dioxide reduction, *Coord. Chem. Rev.*, 2022, **469**, 214664.
- 128 C. M. Yang, M. V. Huynh, T. Y. Liang, *et al.*, Metal-organic framework-derived Mg-Zn hybrid nanocatalyst for biodiesel production, *Adv. Powder Technol.*, 2022, **33**, 103365.
- 129 J. V. L. Ruatpuia, G. Halder, S. Mohan, *et al.*, Microwave-assisted biodiesel production using ZIF-8 MOF-derived nanocatalyst: A process optimization, kinetics,



- thermodynamics and life cycle cost analysis, *Energy Convers. Manage.*, 2023, **292**, 117418.
- 130 N. Y. Lu, X. L. Zhang, X. L. Yan, *et al.*, Synthesis of novel mesoporous sulfated zirconia nanosheets derived from Zr-based metal-organic frameworks, *CrystEngComm*, 2020, **22**, 44–51.
- 131 T. Wang, X. Ma, N. Bingwa, H. Yu, Y. Wang, G. Li, M. Guo, Q. Xiao, S. Li, X. Zhao and H. Li, A novel bimetallic CaFe-MOF derivative for transesterification: Catalytic performance, characterization, and stability, *Energy*, 2024, **292**, 130544.
- 132 Q. Y. Zhang, Q. Z. Luo, X. J. Yang, Y. P. Wu, B. B. Yang, J. L. Wang and Y. T. Zhang, Metal-organic framework-derived nanoporous titanium dioxide-heteropoly acid composites and its application in esterification, *Green Process. Synth.*, 2021, **10**, 284–294.
- 133 Q. Y. Zhang, D. D. Lei, Q. Z. Luo, X. J. Yang, Y. P. Wu, J. L. Wang and Y. T. Zhang, MOF-derived zirconia-supported Keggin heteropoly acid nanoporous hybrids as a reusable catalyst for methyl oleate production, *RSC Adv.*, 2021, **11**, 8117–8123.
- 134 Q. Y. Zhang, M. M. Hu, J. L. Wang, Y. T. Lei, Y. P. Wu, Q. Liu, Y. T. Zhao and Y. T. Zhang, Synthesis of silicotungstic acid/Ni-Zr-O composite nanoparticle by using bimetallic Ni-Zr MOF for fatty acid esterification, *Catalysts*, 2023, **13**, 40.
- 135 Q. Y. Zhang, L. M. Luo, J. X. Jin, Y. P. Wu and Y. T. Zhang, Facile preparation of bimetallic MOF-derived supported tungstophosphoric acid composites for biodiesel production, *Period. Polytech., Chem. Eng.*, 2023, **67**, 337–344.
- 136 F. Wang, Y. Gao, S. Liu, X. Yi, C. Wang and H. Fu, Fabrication strategies of metal-organic frameworks derivatives for catalytic aqueous pollutants elimination, *Chem. Eng. J.*, 2023, **463**, 142466.
- 137 Y. X. Li, Y. C. Han and C. C. Wang, Fabrication strategies and Cr(VI) elimination activities of the MOF-derivatives and their composites, *Chem. Eng. J.*, 2021, **405**, 126648.

